Solid-State Electronics Pergamon Press 1970. Vol. 13, pp. 583–608. Printed in Great Britain

MEASUREMENT OF THE IONIZATION RATES IN DIFFUSED SILICON p–n JUNCTIONS

R. VAN OVERSTRAETEN and H. DE MAN

Electronic Research Laboratories, Section Solid State Electronics, Catholic University of Louvain, 94 Kardinaal Mercierlaan Heverlee, Belgium

(*Received* 26 *May* 1969)

Abstract—An improved method is presented for calculating the ionization rates α_n and α_p from charge multiplication measurements on diffused silicon p–n junctions. The main features of this method are:

The real impurity profile is approximated by an exponential function whose parameters are calculated from capacitance measurements; the ratio $\gamma = \alpha_p/\alpha_n$ as a function of the electric field is calculated from multiplication measurements; the ionization rates are solved from the ionization integral for pure electron injection, taking the influence of the threshold energy into account.

Measurements on narrow junctions agree with measurements on wide junctions by assuming a threshold energy of 1.8 eV for electrons, in agreement with the results of MOLL and VAN OVERSTRAETEN.[1] The ionization rates differ from those of MOLL and VAN OVERSTRAETEN[1] and of LEE, LOGAN *et al.*[2] mainly because these authors neglect the influence of the threshold energy.

The electron and hole data satisfy Chynoweth's law

$$\alpha(E) = \alpha_\infty \exp(-b/|E|), \text{ cm}^{-1}$$

with:

for electrons	α_∞	$= 7.03 \times 10^5$ cm^{-1}
	b	$= 1.231 \times 10^6$ V cm^{-1}
	for	$1.75 \times 10^5 \leqslant E \leqslant 6.0 \times 10^5$ V cm^{-1}
for holes	α_∞	$= 1.582 \times 10^6$ cm^{-1}
	b	$= 2.036 \times 10^6$ V cm^{-1}
	for	$1.75 \times 10^5 \leqslant E \leqslant 4.0 \times 10^5$ V cm^{-1}
and	α_∞	$= 6.71 \times 10^5$ cm^{-1}
	b	$= 1.693 \times 10^6$ V cm^{-1}
	for	$4.0 \times 10^5 \leqslant E \leqslant 6.0 \times 10^5$ V cm^{-1}

Breakdown voltages are computed for high voltage p–n and p–i–n diodes. These are in good agreement with experiments, indicating the reliability of the ionization rates.

Résumé—On présente une méthode améliorée pour calculer les taux d'ionisation α_n et α_p à partir des mesures de multiplication de charge sur des jonctions p–n diffusées en silicium. Les principaux aspects de cette méthode sont:

—les profils d'impureté réels sont approximés par une fonction exponentielle dont les paramètres sont calculés des mesures de capacité.
—le rapport $\gamma = \alpha_n/\alpha_p$ en fonction du champ électrique est calculé des mesures de multiplication.
—les taux d'ionisation sont obtenus de l'intégrale d'ionisation de l'injection d'électrons purs, en tenant compte de l'énergie de seuil.

Les mesures sur les jonctions étroites sont en accord avec les mesures sur les jonctions larges en supposant une énergie de seuil de 1,8 eV pour les électrons en accord avec les résultats de MOLL et VAN OVERSTRAETEN.[1] Les taux d'ionisation diffèrent de ceux de MOLL et VAN OVERSTRAETEN[1] et LEE, LOGAN *et al.*[2] surtout parce que ces auteurs négligent l'influence de l'énergie de seuil.

Les données valeurs obtenues pour les électrons et les trous satisfont la loi de Chynoweth

$$\alpha(E) = \alpha_\infty \exp(-b/|E|) \text{ cm}^{-1}$$

avec:

—pour les électrons $\alpha_\infty = 7{,}03 \times 10^5\ \text{cm}^{-1}$
$b = 1{,}231 \times 10^6\ \text{V cm}^{-1}$
pour $1{,}75 \times 10^5 \leqslant E \leqslant 6{,}0 \times 10^5\ \text{V cm}^{-1}$
—pour les trous $\alpha_\infty = 1{,}582 \times 10^6\ \text{cm}^{-1}$
$b = 2{,}036 \times 10^6\ \text{V cm}^{-1}$
pour $1{,}75 \times 10^5 \leqslant E \leqslant 4{,}0 \times 10^5\ \text{V cm}^{-1}$
et $\alpha_\infty = 6{,}71 \times 10^5\ \text{cm}^{-1}$
$b = 1{,}693 \times 10^6\ \text{V cm}^{-1}$
pour $4{,}0 \times 10^5 \leqslant E \leqslant 6{,}0 \times 10^5\ \text{V cm}^{-1}$

Des tensions de rupture sont calculées pour des diodes p–n et p–i–n à hautes tensions. Celles-ci sont en bon accord avec les expériences indiquant des taux d'ionisation sûrs.

Zusammenfassung—Eine verbesserte Methode zur Berechnung der Ionisationsraten α_n und α_p aus Messungen der Ladungsträgermultiplikation bei diffundierten Silizium-pn-Übergängen wird angegeben. Die wichtigsten Charakteristika der Methode sind:

Das tatsächliche Störstellenprofil wird durch eine Exponentialfunktion angenähert, deren Parameter aus Kapazitätsmessungen berechnet werden.

Das Verhältnis $\gamma = \alpha_p/\alpha_n$ wird als Funktion des elektrischen Feldes aus Multiplikationsmessungen ermittelt.

Die Ionisationsraten werden aus dem Ionisationsintegral bei reiner Elektroneninjektion bestimmt unter Berücksichtigung des Einflusses einer Schwellenenergie.

Messungen an schmalen pn-Übergängen stimmen mit solchen an weiten pn-Übergängen überein unter der Annahme einer Schwellenenergie von 1,8 eV für Elektronen. Dieser Wert ist in Übereinstimmung mit Ergebnissen von MOLL und VAN OVERSTRAETEN.[1] Die Ionisationsrate unterscheidet sich von den Werten dieser Autoren und denen von LEE, LOGAN *et al.*[2] hauptsächlich deshalb, weil diese den Einfluss der Schwellenenergie vernachlässigt haben.

Die Ergebnisse für Elektronen und Löcher erfüllen das Gesetz von Chynoweth

$$\alpha(E) = \alpha_\infty(\exp - b/|E|)(\text{cm}^{-1})$$

mit den Parameterweten:

Für Elektronen $\alpha_\infty = 7{,}03 \cdot 10^5/\text{cm}$
$b = 1{,}231 \cdot 10^6\ \text{V/cm}$
im Bereich $1{,}75 \cdot 10^5 \leqslant E\ (\text{V/cm}) \leqslant 6{,}0 \cdot 10^5$
Für Löcher $\alpha_\infty = 1{,}582 \cdot 10^6/\text{cm}$
$b = 2{,}036 \cdot 10^6/\text{cm}$
im Bereich $1{,}75 \cdot 10^5 \leqslant E\ (\text{V/cm}) \leqslant 4{,}0 \cdot 10^5$
und $\alpha_\infty = 6{,}71 \cdot 10^5/\text{cm}$
$b = 1{,}693 \cdot 10^6/\text{cm}$
im Bereich $4{,}0 \cdot 10^5 \leqslant E\ (\text{V/cm}) \leqslant 6{,}0 \cdot 10^5$

Die Durchbruchsspannungen für Hochspannungs-p–n- und p–i–n-Dioden wurden berechnet. Sie sind in guter Übereinstimmung mit den Experimenten, was die Zuverlässigkeit der ermittelten Werte für die Ionisationsraten anzeigt.

INTRODUCTION

THE IONIZATION rates of silicon have been calculated by several investigators from the charge multiplication in p–n junctions. The most recent and most widely used data are those of MOLL and VAN OVERSTRAETEN[1] and those of LEE, LOGAN *et al.*[2] and are shown in Fig. 1.

The data of MOLL and VAN OVERSTRAETEN (curve 1 for electrons, curve 2 for holes) are obtained from narrow junctions (depletion layer width of the order of 0·3 μm) and are valid in the high electric field range ($3{\cdot}3 \times 10^5 \leqslant E \leqslant 6{\cdot}6 \times 10^5\ \text{V cm}^{-1}$). It will be proved that a correction for the threshold energy for ionization has to be applied for these narrow junctions. These authors solve the ionization integral by an iterative method, assuming the ratio of the ionization rates to be constant. It will be proved that this assumption may be allowed for high electric fields. Indications are also given that their threshold energy $\epsilon_i = 1{\cdot}8$ eV for electrons agrees with our measurements.

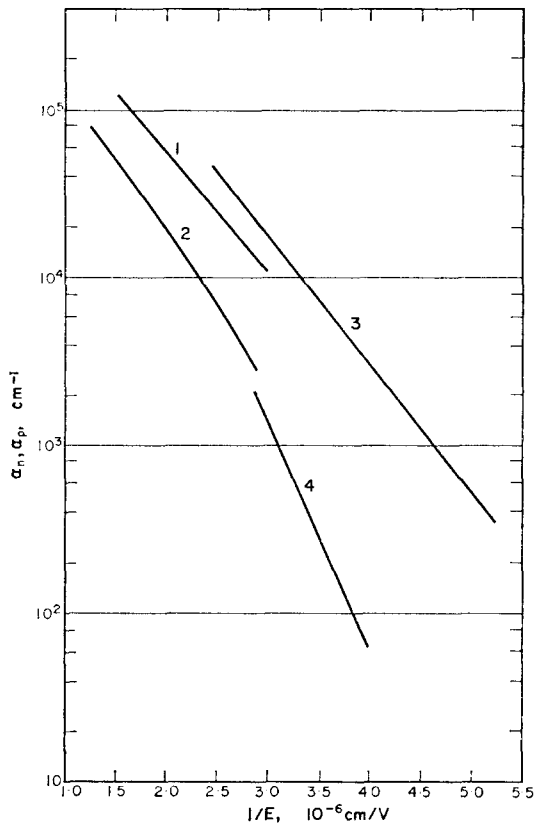

FIG. 1. Ionization rates in function of the reciprocal of the electric field E.

1 and 2: electron- and hole data from MOLL and VAN OVERSTRAETEN.[1]

3 and 4 electron- and hole data from LEE, *et al.*[2].

The data of LEE, LOGAN *et al.*[2] (curve 3 for electrons, curve 4 for holes) are valid for low electric fields ($1{\cdot}8\times10^5 \leqslant E \leqslant 4{\cdot}0\times10^5$ V cm^{-1}). In the intermediate field range ($3{\cdot}3\times10^5 \leqslant E \leqslant 5{\cdot}0\times10^5$ V cm^{-1}) the electron data differ by 40 per cent with those of MOLL and VAN OVERSTRAETEN. About these data there is also some doubt for two reasons:

(1) The ionization rates derived from diode unit 29–9[2] are shown to be incompatible with the measured multiplication data.

(2) For their diode 6 AG 35, with a breakdown voltage of 6 V, the influence of threshold energy was neglected.

Further, KOKOSA and DAVIES[3] have shown that these data are incompatible with breakdown voltages of abrupt p–n junctions above 500 V. Therefore breakdown voltages are calculated with the new ionization rates giving at the same time practical curves especially for high voltage devices and, by their good agreement with measurements, a verification of the ionization rates.

The method for measuring ionization data, to be presented here, tries to use better appoximations than those used by former investigators. The main differences are:

(1) The real impurity profile is approximated by an exponential function. The validity of this approximation will be proved experimentally using capacitance measurements.

(2) The ionization ratio $\gamma = \alpha_p/\alpha_n$ is calculated as a function of the electric field E from electron and hole initiated multiplication factors measured on the same diode.

(3) The ionization integral for pure electron injection is solved on a computer, taking the influence of the threshold energy ϵ_i into account, and using a least square method minimizing the error between the ionization integral and measured multiplication factor.

Our measurements obtained from narrow and wide junctions are in complete agreement. The electron data satisfy Chynoweth's law in the field range $1{\cdot}75\times10^5 \leqslant E \leqslant 6{\cdot}0\times10^5$ V cm^{-1}.

In Section 1 the measurement method of the ionization rates is discussed. In Section 2 the new results are given and discussed, while in Section 3 breakdown voltages for p–n and p–i–n junctions, calculated with the new data are discussed and are compared with experiments and with previous calculations.

1. MEASUREMENT OF THE IONIZATION RATES α_n AND α_p

1.1 *Statement of the problem*

Let us consider the reverse biased junction, schematically shown in Fig. 2. The origin of the x-axis is taken at the metallurgical junction. The boundaries of the depletion layer are respectively x_n and x_p. The total voltage across the junction is:

$$V = V_a + V_d$$

with V_a the external applied voltage and V_d the built-in potential. The sign convention for V_a used here, is that V_a is positive for reverse bias.

The currents considered here to measure the multiplication factor, result from external excitation (for example from light shone on the junction).

The minority carrier currents are referred to as J_{pn}, the hole current at x_n and J_{np}, the electron current at x_p respectively. For $qV = q(V_a+V_d)$ much larger than the threshold energy for ionization ϵ_i, the electrons and holes ionize, resulting in an increase of J_{pn} to J_{pp} at x_p and of J_{np} to J_{nn} at x_n. Since for $V_a = 0$ the total voltage across the junction corresponds to an energy, qV_d, which is smaller than the threshold energy ϵ_i, there is no ionization. Consequently, the multiplication factor at a reverse voltage V may be defined and is calculated as:[2]

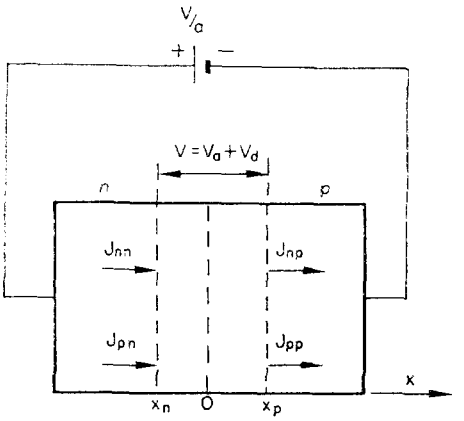

FIG. 2. Diode model and symbols used for the calculation of the multiplication factors.

$$M(V) = \frac{J(V)}{J(V_d)} = \frac{J_{nn}+J_{pn}}{J_{np}+J_{pn}} = \frac{J_{pp}+J_{np}}{J_{pn}+J_{np}}$$

$$= \frac{\exp\left[-\int_{x_n}^{x_p}(\alpha_n-\alpha_p)\,dx\right]+k}{(1+k)\left\{1-\int_{x_n}^{x_p}\alpha_n \exp\left[-\int_{x}^{x_p}(\alpha_n-\alpha_p)\,dx'\right]dx\right\}} \tag{1a}$$

$$= \frac{k\exp\left[\int_{x_n}^{x_p}(\alpha_n-\alpha_p)\,dx\right]+1}{(1+k)\left\{1-\int_{x_n}^{x_p}\alpha_p \exp\left[\int_{x_n}^{x}(\alpha_n-\alpha_p)\,dx'\right]dx\right\}}, \tag{1b}$$

with $k = J_{np}/J_{pn}$ the *injection ratio*. (2)

For pure hole injection, $k = 0$ and

$$1-\frac{1}{M_p(V)} = \Phi_p(V) = \int_{x_n}^{x_p}\alpha_p \exp\left[\int_{x_n}^{x}(\alpha_n-\alpha_p)\,dx'\right]dx. \tag{3}$$

For pure electron injection, $k = \infty$ and

$$1 - \frac{1}{M_n(V)} = \Phi_n(V) = \int_{x_n}^{x_p} \alpha_n \times \exp\left[- \int_{x}^{x_p} (\alpha_n - \alpha_p)\, dx' \right] dx. \quad (4)$$

$M_n(V)$ and $M_p(V)$ are the multiplication factors, respectively for pure electron and for pure hole injection; $\Phi_n(V)$ and $\Phi_p(V)$ are referred to as the reduced multiplication factors. The expressions (3) and (4) are referred to as the ionization integrals.

The problem consists of solving the integral equations (3) and (4) with respect to $\alpha_n(E)$ and $\alpha_p(E)$ after having measured $M_p(V)$ and $M_n(V)$ on a given diode. The determination of $\alpha_n(E)$ and $\alpha_p(E)$ can thus be divided into three parts:

(1) The determination of the diode parameters $x_p(V)$, $x_n(V)$ and $E(x,V)$ (Section 1.2).

(2) The measurement of the multiplication factors $M_p(V)$ and $M_n(V)$ (Section 1.3).

(3) The determination of the ionization rates from the multiplication factors $M_n(V)$ and $M_p(V)$ by solving the ionization integrals (Section 1.4).

1.2 *Determination of* $x_p(V)$, $x_n(V)$, *and* $E(x, V)$

1.2.a *Impurity profile approximation.* In Ref. 4 it is shown that, in the depletion region, the net impurity profile can be approximated fairly accurately by an exponential profile given by:

$$N(x) = N_s[\exp(-x/\lambda) - 1] \quad (5)$$

with (Fig. 3)($N(x)$: the net impurity concentration (donor minus acceptor concentration)

x: the distance coordinate (origin at the metallurgical junction)

N_s: the substrate impurity concentration in almost all cases[4]

λ: a distance parameter, which may be determined by capacitance measurements and which is related to the absolute value of the gradient of the impurity profile in the origin by

$$a = N_s/\lambda \quad (5a)$$

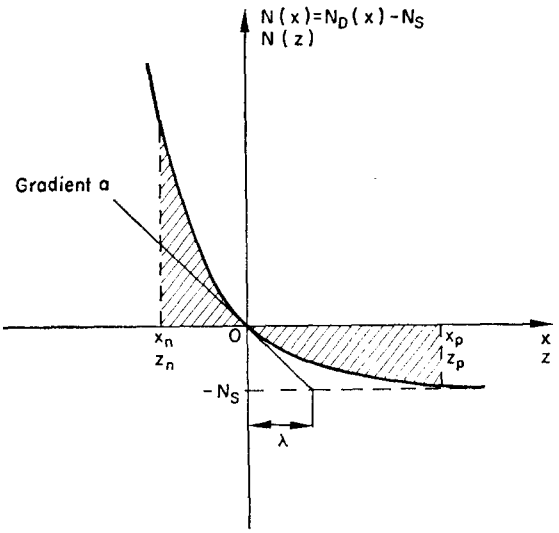

FIG. 3. Model of the depletion region for an exponential profile.

This simple exponential approximation is used for two reasons:

(a) If the parameters N_s and λ (or the gradient a) are determined by capacitance measurements, equation (5) is shown to be a very good approximation in the depletion region.[4] This will be proved in section 1.2.c.

(b) The exponential profile with N_s and λ determined by capacitance measurements is, in the depletion region, a better approximation for the real profile than the complementary error function or than the Gauss-function computed from theoretical diffusion parameters. It is shown[5] that, especially for shallow diffusions, the real profile differs quite strongly from these theoretical profiles.

1.2.b *Solution of Poisson's equation for the exponential approximation.* Introducing the reduced distance:

$$z = x/\lambda, \quad (6)$$

it can be shown[4] that a double integration of Poisson's equation yields the following set of two equations in the reduced partial widths z_p and

z_n (Fig. 3) of the depletion region:

$$\begin{cases} F(z_n) = F(z_p) & (7) \\ \exp(-z_n)(z_p - z_n - 1) + \\ \qquad \exp(-z_p) - (z_p - z_n)^2/2 = v & (8) \end{cases}$$

with:

$$F(z) = \exp(-z) + z - 1 \quad (9)$$

$$v = (V_a + V_d)/\lambda E_0, \text{ the reduced potential} \quad (10)$$

and with:

$$E_0 = q\lambda N_s/\epsilon. \quad (11)$$

Herein is q the electronic charge and ϵ the permittivity of silicon taken as $\epsilon = 1{\cdot}04 \times 10^{-12}$ F/cm.[6]

The electric field E is given by:

$$E(z) = E_0[F(z_n) - F(z)], \quad (12)$$

while the maximum electric field E_m is obtained for $z = 0$:

$$E_m = E_0 F(z_n). \quad (13)$$

Knowing N_s and λ, the widths z_p and z_n can be solved numerically from equation (7) and (8) for a given V_a. The electric field $E(z,V)$ and its maximum value $E_m(V)$ can then be calculated from (12) and (13). Going back to the original coordinate x, gives the required $x_p(V)$, $x_n(V)$ and $E(x, V)$. The method to deduce N_s λ and V_d from capacitance measurements will be discussed now.

1.2.c *Verification of the exponential approximation by capacitance measurements.* The differential capacitance of diffused mesa diodes behaves typically as shown in Figs. 4 and 5. In Fig. 4, measurements of C^{-3} vs. V_a are plotted in the voltage range $-0{\cdot}5 \leqslant V_a \leqslant 0{\cdot}2$ V. for diode D III 1, one of the diodes used in our experiments. This plot yields a linear relation between C^{-3} and V_a.

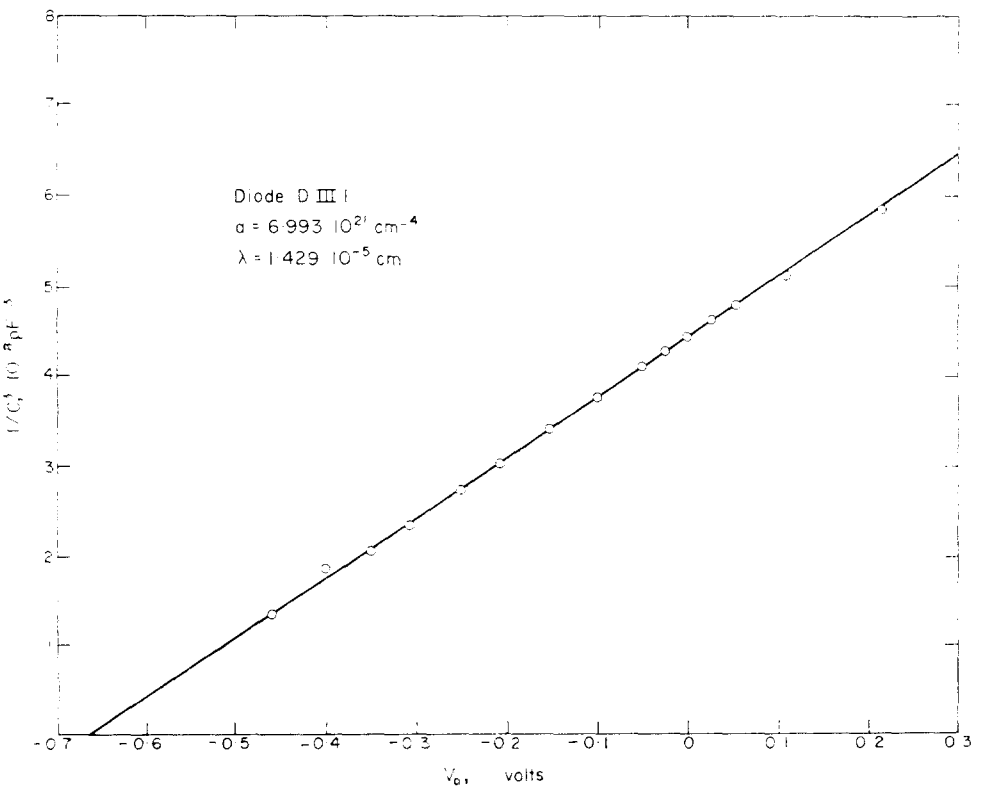

FIG. 4. $1/C^3$ in function of the voltage V_a for $-0{\cdot}5 \leqslant V_a \leqslant +0{\cdot}2$ V for diode D III 1.

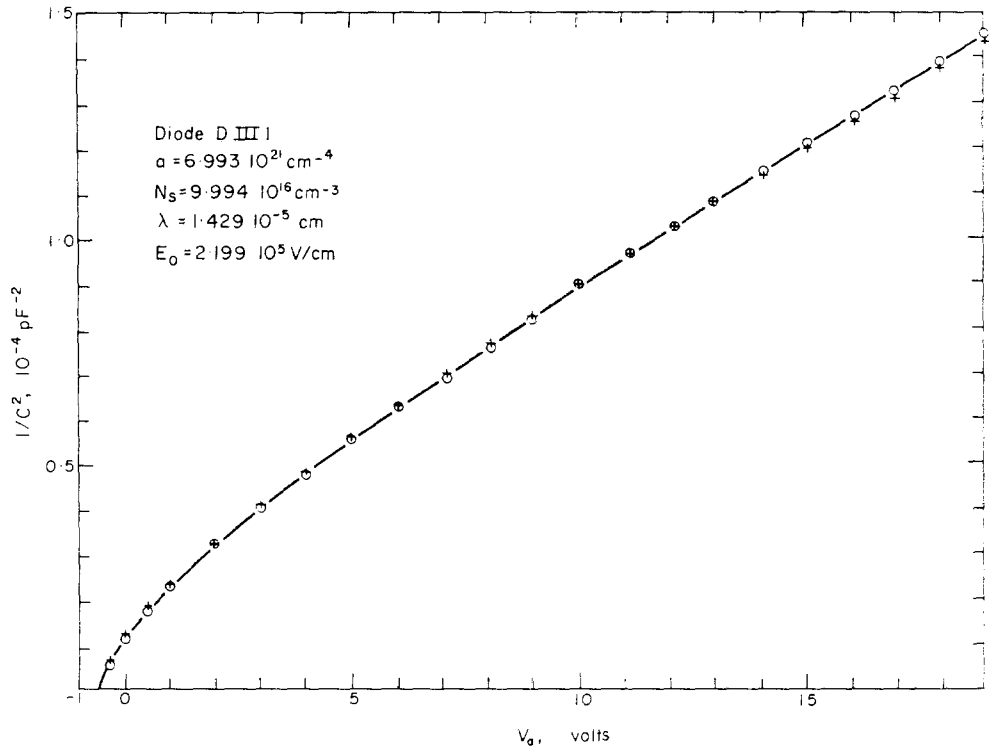

FIG. 5. $1/C^2$ in function of the voltage V_a for diodeD III 1.
+ computed from the exponential approximation
○ measurements

This indicates that the depletion region extends only slightly around the metallurgical junction where the profile is nearly linear. The intersection of the $C^{-3}(V_a)$ line with the V_a- axis gives the built-in voltage V_d. Figure 5 shows C^{-2} vs. V_a in the whole voltage range up to about the breakdown voltage (20·5 V). For $V_a > 10$ V, C^{-2} vs. V_a gives a straight line. This means that the depletion region extends mainly into the substrate. In this voltage range, the capacitance thus depends strongly on N_s (abrupt behavior). For $0{\cdot}2 < V_a < 10$ V, the profile has neither a linear nor an abrupt behavior. The way in which the exponential approximation is verified will be described now.

For a given bias V_{ak}, the differential capacitance C_k of a diode with area A and with an exponential impurity profile, is given by:

$$C_k = \frac{\epsilon A}{w_k} = \frac{\epsilon A}{\lambda[z_p(v_k) - z_n(v_k)]}, \qquad (14)$$

wherin w_k is the total width of the depletion region. From equation (10) and (11) v_k is given by:

$$v_k = (V_{ak} + V_d)/\lambda E_0 = (V_{ak} + V_d)/q\lambda^2 N_s. \quad (15)$$

z_p and z_n are solutions of (7) and (8) at the given value of v_k. Thus one can write:

$$C_k = C_k(\lambda, N_s). \qquad (16)$$

Let C_{mk} be the measured capacitance at the same voltage V_{ak}. The capacitances are measured for l different voltages V_{ak}. The most appropriate values of N_s and λ can be determined by minimizing the mean square deviation Δ between $C_k(\lambda, N_s)$ and C_{mk}, given by:

$$\Delta(\lambda, N_s) = \frac{1}{l} \sum_{k=1}^{l} \left[\frac{C_{mk} - C_k(\lambda, N_s)}{C_{mk}} \right]^2 \qquad (17)$$

The function $\Delta(\lambda, N_s)$ is programmed on a

computer and minimized with respect to λ and N_s. Usually about forty measurements are made, fifteen of which are between $-0{\cdot}5$ and $+0{\cdot}2$ V. This procedure usually gives a fit of the computed and measured values to within 1 per cent, being of the same order as the experimental error (see also Figs. 4 and 5).

This procedure may thus be considered as an experimental verification of the exponential approximation, and gives at the same time the values of N_s and λ. It may be remarked also that the so determined substrate concentration N_s agrees very well with the value N_{sr} determined by resistivity measurements on the substrate (see Table 3, discussed later).

1.2.d. *Conclusion.* The method described in this section gives an accurate determination of the profile parameters N_s and λ. These yield:

$$x_p = \lambda z_p(v)$$
$$x_n = \lambda z_n(v)$$
$$E(z) = E_0[F(z_n) - F(z)].$$

1.3 *Measurement of the multiplication factors $M_n(V)$ and $M_p(V)$.*

The set-up for multiplication measurements is shown in Fig. 6. The diode D is a phosphorus diffused mesa diode with a high surface concentration (10^{20} cm^{-3}), allowing a direct tungsten probe contact. At the p-side a Au–Ga contact is evaporated. The diode is reverse biased using a voltage source V_a in series with a load resistance of 100 Ω. An alternating photocurrent J is generated by illuminating the diode through the microscope M, by chopped light with a wavelength determined by the optical filter F. The photocurrent J gives rise to a voltage signal across the 100 Ω resistor. This signal is amplified using a HP 1403 A oscilloscope amplifier, rectified in R and measured as a voltage V_f, proportional to J, using a Solartron digital voltmeter DVM. Measurement of the photocurrent $J(V) = J(V_a + V_d)$ and of the photocurrent $J(V_d)$ at zero bias gives the multiplication factor:

$$M(V) = J(V)/J(V_d).$$

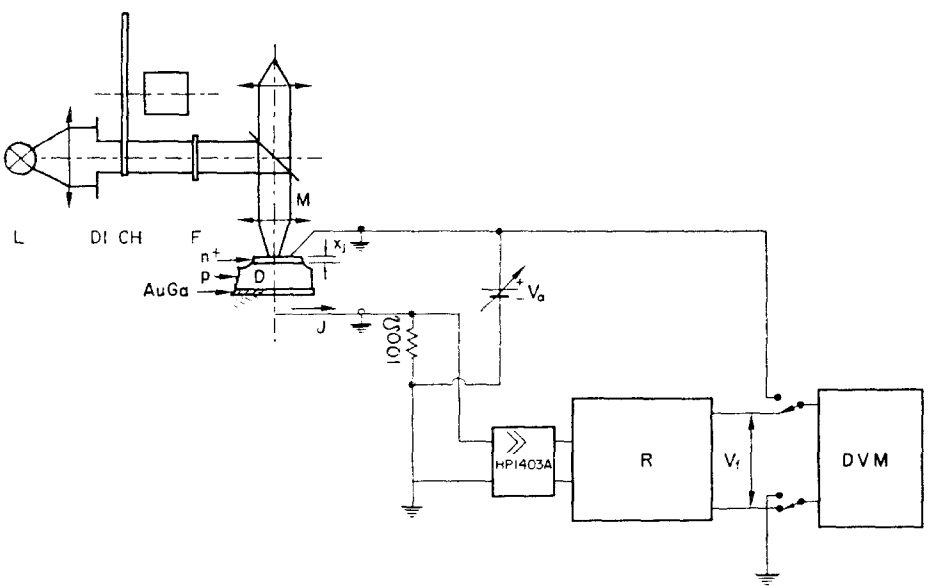

FIG. 6. Set up for measuring the multiplication factors $M_n(V)$ and $M_p(V)$.

D	: diode	M	: Microscope
DI	: diaphragm	HP 1403	: a.c. amplifier
CH	: light-chopper	R	: rectifier network
F	: optical filter	DVM	: digital voltmeter

Since the penetration depth of light in Silicon is strongly dependent on the lightwavelength[7] it is evident that an appropriate choice of the latter and of the diffusion depth x_j of the diode permits us to obtain nearly pure hole or nearly pure electron injection, as will be discussed in more detail in Section 1.4.

1.4 *Determination of the ionization rates from the multiplication factors*

1.4.a *Principle of the solution. Correction for the threshold energy* ϵ_i. A simultaneous solution of the ionization integrals (3) and (4) presents serious mathematical difficulties. In the next section it will be shown that it is possible to derive the ratio

$$\gamma(E) = \alpha_p(E)/\alpha_n(E) \tag{18}$$

from the measurement of $M_n(V)$ and $M_p(V)$ on the same junction. With (18) the ionization integral (4) becomes

$$\Phi_n(V) = \int_{x_n}^{x_p} \alpha_n(E) \times \exp\Big[-\int_x^{x_p} (1-\gamma(E))\alpha_n(E)\,dx'\Big]\,dx. \tag{19}$$

Knowing $\gamma(E)$ the problem is reduced to solving equation (19) with respect to $\alpha_n(E)$. $\alpha_p(E)$ is then given by:

$$\alpha_p(E) = \alpha_n(E)\,.\,\gamma(E).$$

Before discussing the determination of $\gamma(E)$, it should be remarked that equation (19) is valid for wide junctions only, where charge multiplication is measurable only for

$$q(V_a + V_d) \gg \epsilon_i$$

with ϵ_i the electron threshold energy for ionization. Therefore a model will be proposed to account for the influence of the threshold energy if $q(V_a+V_d)$ is only slightly higher than ϵ_i (Fig. 7). Assume pure electron injection ($J_{pn} = 0$). The distance $(x_p - x_i)$ to be covered by the electron current J_{np} injected into x_p, before ionization becomes possible, is given by

$$\psi(x_i) - \psi(x_p) = \int_{x_i}^{x_p} E(x)\,dx = \frac{\epsilon_i}{q}. \tag{20}$$

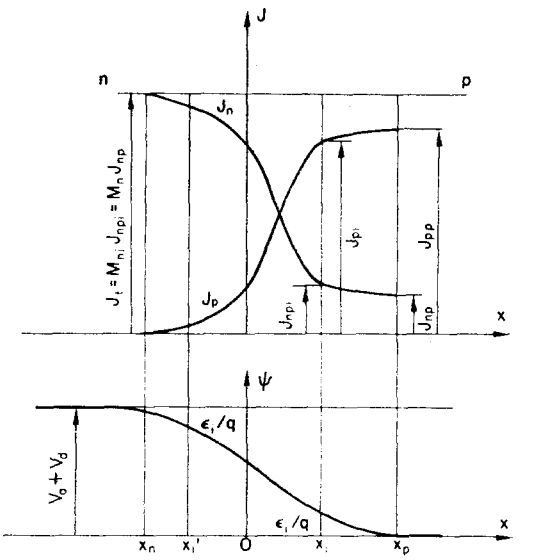

FIG. 7. Model for the calculation of the influence of the threshold energy ϵ_i on the charge multiplication.

with $\psi(x_i)$ and $\psi(x_p)$ the crystal potentials respectively at x_i and at x_p.

For $x < x_i$, the ionization integral (4) may be used. The holes injected from left to right at x_i generate electron-hole pairs by secondary ionization and increase the electron current at x_i to J_{npi}, larger than J_{np}.

The multiplication in the region (x_n, x_i) is thus given by:

$$\phi_{ni} = 1 - \frac{1}{M_{ni}} = \int_{x_n}^{x_i} \alpha_n \times \exp\Big[-\int_x^{x_i} (1-\gamma)\,\alpha_n\,dx'\Big]\,dx. \tag{21}$$

with x_i given by (20).*

* Although between a position x_i' and x_n, no new secondary electrons are generated by those entering at x_i' with an energy $\epsilon = 0$, the integral is taken from x_n to x_i. This is justified since the electric field between x_i' and x_n is much lower than between x_i' and x_i and the contribution to J_n due to the electrons entering at x_i' with energy $\epsilon = 0$ is very small. Taking the integral from x_n to x_i gives thus a very small overestimation of J_n, which is neglected here.

The total electron current at x_n becomes

$$J_t = M_n J_{np} = M_{ni} J_{npi} \tag{22}$$

with M_n the *measured* value of the multiplication factor. The electron current at x_i may be written

$$J_{npi} = J_{np} + J_{pi} \int_{x_i}^{x_p} \alpha_p \, dx$$
$$= J_{np} + J_{pi} \int_{x_i}^{x_p} \gamma \alpha_n \, dx \tag{23}$$

with J_{pi} the hole current in x_i, given by:

$$J_{pi} = J_t - J_{npi} = (M_{ni} - 1) J_{npi}, \tag{24}$$

using (22).
With (24), equation (23) yields:

$$J_{npi} = J_{np} + (M_{ni} - 1) J_{npi} \int_{x_i}^{x_p} \gamma \alpha_n \, dx \tag{25}$$

With (25), (22) yields:

$$M_n \left[1 - (M_{ni} - 1) \int_{x_i}^{x_p} \gamma \alpha_n \, dx \right] = M_{ni} \tag{26}$$

or after some manipulation:

$$\Phi_n = 1 - \frac{1}{M_n} = \left(1 - \frac{1}{M_{ni}} \right) \left(1 + \int_{x_i}^{x_p} \gamma \alpha_n \, dx \right) \tag{27}$$

and with (21):

$$\Phi_n(V) = \left\{ 1 + \int_{x_n}^{x_p} \gamma(E) \alpha_n(E) \, dx \right\} \left\{ \int_{x_n}^{x_i} \alpha_n(E) \times \exp\left[- \int_{x_n}^{x_i} \alpha_n(E) [1 - \gamma(E) \, dx'] \right] dx \right\}. \tag{28}$$

This equation represents the ionization integral for pure electron injection, corrected for the threshold energy of electrons. It should be remarked that for wide junctions, the electric field and thus $\alpha_n(E)$ are low for $x_i < x < x_p$, and equation (28) becomes identical to equation (19).

1.4.*b Calculation of $\gamma(E)$ from $M_p(V)$ and $M_n(V)$ and general procedure to determine $\alpha_n(E)$ and $\alpha_p(E)$*

General procedure. The solution of the ionization integral (28) requires the knowledge of $\gamma(E) = \alpha_p(E)/\alpha_n(E)$. To discuss the method for determining $\gamma(E)$, we first suppose γ to be independent of

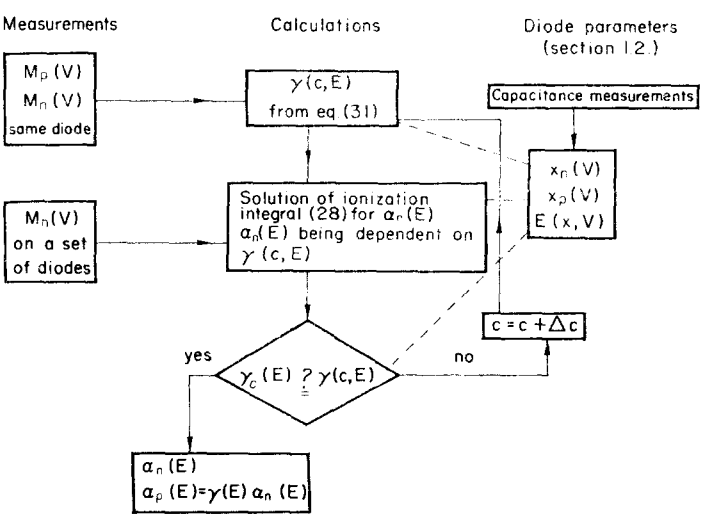

FIG. 8. Iteration scheme for the calculation of $\alpha_n(E)$ and $\alpha_p(E)$ from multiplication measurements.

the electric field. In this case, the integrals (3) and (4) become:

$$1-\frac{1}{M_n(V)}=\frac{1}{\gamma-1}\left\{\exp\left[-(1-\gamma)\int_{x_n}^{x_p}\alpha_n\,dx\right]-1\right\} \tag{29}$$

$$1-\frac{1}{M_p(V)}=\frac{\gamma}{\gamma-1}\left\{1-\exp(1-\gamma)\int_{x_n}^{x_p}\alpha_n\,dx\right\} \tag{30}$$

Elimination of

$$\int_{x_n}^{x_p}\alpha_n\,dx$$

yields:

$$\gamma=\frac{M_p(V)-1}{M_n(V)-1}. \tag{31}$$

γ can thus be calculated from the measurements of $M_p(V)$ and $M_n(V)$ on the same diode at the same voltage V. The value of γ calculated from (31) depends strongly on V, indicating that γ depends on the electric field, contrary to the assumption leading to (31). However, since the ionization rates α_p and α_n show an exponential dependence on the electric field E, it is clear that the important contribution to the kernel of the ionization integral comes from fields close to the maximum electric field E_m in the junction. Therefore the constant γ may be associated with an electric field $E=cE_m$ with c close to unity. The unknown constant c can be determined by an iterative procedure described schematically in Fig. 8. This procedure also gives us $\alpha_n(E)$ and $\alpha_p(E)$. Taking a first estimate for c, the ratio $\gamma(c, E)$ is calculated with (31) from measurements of $M_n(V)$ and $M_p(V)$ on the same diode. The symbol $\gamma(c, E)$ is used indicating that γ depends on c. The second step consists in solving the ionization integral (28) for $M_n(V)$ values measured on a set of diodes and using the given $\gamma(c, E)$ function. This gives a first estimate for $\alpha_n(E)$ and $\alpha_p(E)=\gamma\alpha_n(E)$ depending on c. Using these $\alpha_n(E)$ and $\alpha_p(E)$, (3) and (4) yield values for $M_n(V)$ and $M_p(V)$. Equation (31) gives a new computed value $\gamma_c(E)$. The criterion for the constant c is that these $\gamma_c(E)$ values must be the same as the values $\gamma(c, E)$. An iteration procedure is used until computed and measured γ values agree. In appendix A it is graphically shown that $c=0{\cdot}9$ is a reasonable value. Therefore, we shall use this value from now on.

Measurement of $\gamma(E)$. The measurement of $M_n(V)$ and $M_p(V)$ is described in Section 1.3. The diffusion depths x_j of the diodes are between 3·5 and 5·5 μm. The diodes are illuminated with chopped i.r. light (tungsten source with Silicon filter of 100 μm thickness) or with light of wavelength of 0·55 μm. Infrared light penetrates deep into the diode and generates mainly an electron current. The light with wavelength of 0·55 μm is absorbed mainly in the surface layer, resulting mainly in a hole injection. For pure electron injection and for pure hole injection, we would measure respectively M_n and M_p. Since, in spite of all precautions one never gets a pure one carrier injection, one necessarily has to calculate with a mixed injection. The measured multiplication factor obtained with the infrared light experiment will be referred to as M_e different from M_n, and the measured multiplication factor obtained with the 0·55 μm experiment will be referred to as M_h different from M_p. $M_e(V)$ and $M_h(V)$ respectively correspond to a finite injection ratio $k=J_{np}/J_{pn}$ and $k'=J_{pn}/J_{np}$. In appendix B, it is shown that in this case, equation (31) for γ can be written as:

$$\gamma=\frac{k(1+k')M_h-(1+k)M_e-kk'+1}{k'(1+k)M_e-(1+k')M_h-kk'+1} \tag{32}$$

The injection ratios k and k' are calculated using the diode model schematically shown in Fig. 9.

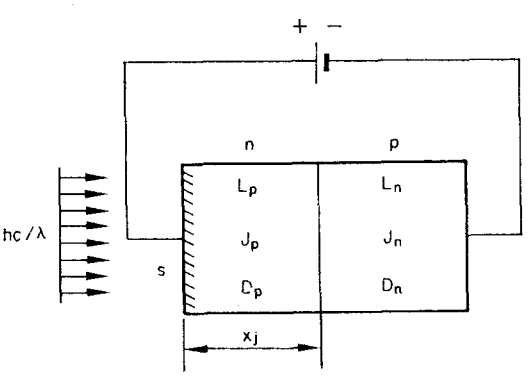

FIG. 9. Diode model for the calculation of the injection ratio k.

The n-side of the junction is illuminated with light of wavelength λ and absorption coefficient α. The lifetime and diffusion lengths in the n- and p-layer are respectively τ_n, L_n and τ_p, L_p. The surface recombination velocity is referred to as s. The absorption law and the diffusion equation from the impurity concentration.[9] The parameters $\beta_{p,n} = (D_{p,n}\tau_{p,n})^{-1/2}$ are calculated. The absorption coefficient for infrared light α_i is much smaller than $10^2\ \mathrm{cm}^{-1}$.[7] Since $\alpha_i \ll \beta_p$, β_n and $\alpha_i x_j \ll 1$, α_i may be neglected in (33). This results in:

$$k = \frac{\beta_p \cosh\beta_p x_j}{\beta_n\{\sinh\beta_p x_j - [s(\cosh\beta_p x_j - 1)/(v_{p0}\cosh\beta_p x_j + s\sinh\beta_p x_j)]\}}$$

give:

$$k = \frac{J_{np}}{J_{pn}} = (\alpha^2 - \beta_p{}^2)e^{-\alpha x_j}\cosh\beta_p x_j/(\alpha+\beta_n) \times \left\{\frac{\alpha v_{p0}\cosh\beta_p x_j + s\beta_p(\cosh\beta_p x_j - e^{-\alpha x_j})}{\alpha v_{p0}\cosh\beta_p x_j + s\alpha\sinh\beta_p x_j} - e^{-\alpha x_j}\left(\cosh\beta_p x_j + \frac{\beta_p}{\alpha}\sinh\beta_p x_j\right)\right\}^{-1} \quad (33)$$

where

$$\beta_{p,n} = \frac{1}{L_{p,n}}$$

and

$$v_{p0} = D_p/L_p.$$

One measurement will be discussed here in detail. The diode parameters are listed in table 1. N_s, λ and V_d are determined from capacitance measurements as discussed in Section 1.2.*c*. The effective electron lifetime τ_n in the substrate is measured using the method described in Ref. 8. It is well known that due to the phosphorus diffusion, the hole lifetime τ_p generally is one or two orders of magnitude smaller than the electron lifetime τ_n. The built-in electric field due to the diffusion profile gives an effective diffusion length 5 to 6 times larger than the real one. Since $L_p = (\sqrt{D_p\tau_p})$, the change in τ_p by the diffusion may, to a first approximation, be regarded as compensated by the change in L_p due to the built-in electric field. We thus take $\tau_p = \tau_n$. With this condition we find, for the diodes we use, that the effective diffusion length L_p exceeds the diffusion depth x_j and one can compute from (33) that in this case k is very insensitive to the value of L_p. The approximation $\tau_n = \tau_p$ is thus sufficient for calculating the injection ratios k and k'. The diffusion constants D_p and D_n are determined

Table 1. Diode parameters of diode γ_{33} for the calculation of the injection ratio k for electron-injection and k' for hole-injection.

	Diode γ_{33}
x_j	4·2 μm
N_s	$3{\cdot}25\times10^{15}\ \mathrm{cm}^{-3}$
λ	$2{\cdot}03\times10^{-5}$ cm
V_d	0·550 V
$\tau_p = \tau_n$	0·49 μsec
D_n	$31{\cdot}2\ \mathrm{cm}^2\ \mathrm{sec}^{-1}$
D_p	$3{\cdot}9\ \mathrm{cm}^2\ \mathrm{sec}^{-1}$
β_n	$2{\cdot}55\times10^2\ \mathrm{cm}^{-1}$
β_p	$7{\cdot}24\times10^2\ \mathrm{cm}^{-1}$
v_{p0}	$2{\cdot}82\times10^3\ \mathrm{cm\ sec}^{-1}$
α_i	$\approx 0\ \mathrm{cm}^{-1}$
α_u	$8\times10^3\ \mathrm{cm}^{-1}$
k_1	11·7
k_2	13·1
k	12·5
k_1'	22·5
k_2'	17·1
k'	19·8

The surface recombination velocity for an etched and diffused Si-surface is estimated to lie between $2{\cdot}10^3\ \mathrm{cm\ sec}^{-1}$ and $10^4\ \mathrm{cm\ sec}^{-1}$.[10] The value used for k is the mean value between k_1 and k_2 respectively calculated for $s = 2\times10^3$ and $s = 10^4\ \mathrm{cm\ sec}^{-1}$. We find $k = 12{\cdot}5$. The absorption coefficient α_u for light with wavelength 0·55 μm is equal to $\alpha_u = 8\times10^3\ \mathrm{cm}^{-1}$[7]; This gives $k' = k^{-1} = 19{\cdot}8$ again obtained by interpolation between k'_1 and k'_2 respectively for $s = 2\times10^3$ and $s = 10^4\ \mathrm{cm\ sec}^{-1}$.

Table 2 gives as a function of the applied bias, the measured hole multiplication factor M_h, the electron multiplication factor M_e, the ionization ratio γ calculated from (32) and the corresponding

Table 2. Measured charge multiplications $M_e(V_a)$ and $M_h(V_a)$, γ values calculated from (61) and associated field $0{\cdot}9\,E_m$ as a function of the diode bias for diode γ_{33}.

V_a V	M_h	Diode γ_{33} M_e	γ	$0{\cdot}9\,E_m$ 10^5 V/cm
60	1·040	1·43	0·0405	1·920
65	1·055	1·61	0·0385	2·010
70	1·090	1·83	0·0557	2·100
75	1·120	2·18	0·0495	2·175
80	1·190	2·62	0·0683	2·245
85	1·270	3·17	0·0706	2·320
90	1·380	4·05	0·0716	2·395
95	1·570	5·27	0·0802	2·410
100	1·860	7·24	0·0850	2·540
105	2·220	9·55	0·0890	2·610
110	2·910	14·33	0·0900	2·670
$k = 12{\cdot}5$			$k' = 19{\cdot}8$	

electric field $E = cE_m$ with $c = 0{\cdot}9$ as explained above. Five other diodes with different breakdown voltages and thus different electric field ranges were studied the same way. The results for $\gamma(E)$ are shown in Fig. 10. The relatively high spread of the results is explained by the high inaccuracy of the measurements necessary at low multiplication factors. Since the results for the several diodes join rather well, they may be considered as sufficiently reliable to approximate them by the curve shown in Fig. 10, or by the analytical expression with

$$\gamma = \Gamma_i \exp(-\beta_i/|E|),\ i = 1, 2 \qquad (34)$$

$$\Gamma_1 = 0{\cdot}955\ \beta_1 = 4{\cdot}62 \times 10^5\ \text{V/cm for } E > 4 \times 10^5\ \text{V/cm}$$

$$\Gamma_2 = 2{\cdot}25\ \beta_2 = 8{\cdot}05 \times 10^5\ \text{V/cm for } E < 4 \times 10^5\ \text{V/cm}.$$

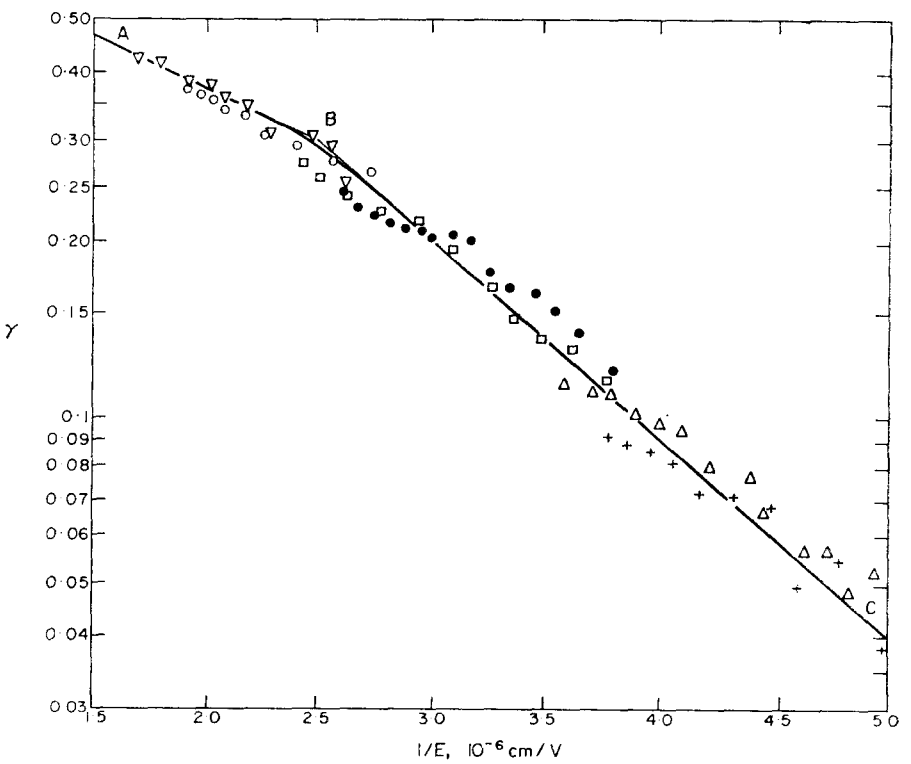

FIG. 10. The ionization ratio $\gamma = \alpha_p/\alpha_n$ in function of the reciprocal of the electric field. The different points correspond to measurements on different diodes.

In the field range used in Ref. 1 ($3{\cdot}3\times10^5 < E < 6{\cdot}6\times10^5$ V-cm^{-1}) γ varies between 0·21 and 0·45. This may be the reason why MOLL and VAN OVERSTRAETEN[1] find a 'mean' value $\gamma = 0{\cdot}33$ without using precise computer calculations. For $E < 4\times10^5$ V-cm^{-1} γ decreases very fast to give $\gamma = 0{\cdot}04$ at $E = 2\times10^5$ V-cm^{-1}. The fast decrease corresponds with the results of LEE, LOGAN, *et al.*[2] However they suggest still lower values.

1.4.*c* *Numerical procedure for the solution of* $\alpha_n(E)$. $M_n(V)$ is measured at m different junction voltages $v = V_a + V_d$ and the diode parameters λ and E_0 are determined as described in Section 1.2. The measurements were made on shallow diffused n^+p ($x_j \leqslant 0{\cdot}5\,\mu$m) diodes and using deep penetrating infrared light. The injection ratio will thus be very large and no correction is needed for hole contamination. Using the subscript k for the kth measurement one calculates the reduced voltage using (10), the normalized junction boundaries z_{pk} and z_{nk} using (7, 8), the electric field in the junction from (12), and the maximum electric field from (13).

Using the normalized coordinate $z = x/\lambda$, the ionization integral (28) reads:

$$\Phi_n(V_k) = \lambda\Big[1+\lambda\int_{z_{ik}}^{z_{pk}}\gamma(E_k)\,\alpha_n(E_k)\,\mathrm{d}z\Big] \times\Big[\int_{z_{nk}}^{z_{ik}}\alpha_n(E_k)\exp\Big\{-\int_{z}^{z_{ik}}\alpha_n(E_k) \times(1-\gamma(E_k))\,\mathrm{d}z'\Big\}\,\mathrm{d}z\Big]. \tag{35}$$

Since $\gamma(E_k)$ is known, the only unknown parameter, except for $\alpha_n(E_k)$. in the right term of (35) is z_{ik}. For the kth measurement this parameter is solved from (20) which for normalized coordinates and with (12) can be written as:

$$q\lambda\int_{z_{ik}}^{z_{pk}}E_0[F(z_{nk})-F(z)]\,\mathrm{d}z = \epsilon_i \tag{36}$$

This transcendental equation in z_{ik} is solved numerically for each measurement and for a given value of ϵ_i using a Gauss quadrature and Müllers-S-iteration method.[11] For ϵ_i we take $\epsilon_i = 1{\cdot}8$ eV corresponding with Ref. 1. Other values have also been taken (see discussion in Section 2).

The problem now is reduced to finding the function $\alpha_n(E_k)$ such that (35) is satisfied for all measurements. In order to simplify this problem we assume that the electron ionization rate $\alpha_n(E)$ satisfies Chynoweth's law:

$$\alpha_n(E) = \alpha_{n\infty}\,\mathrm{e}^{-b_n/|E|} \tag{37}$$

in the field range corresponding to the measured diode. In (37) $\alpha_{n\infty}$ and b_n are constants which must be adjusted to satisfy (35) in all measured points. This assumption is justified as follows:

Previous measurements on Silicon[1,2] and Germanium[12] yield this field dependence of $\alpha_n(E)$ over a considerable field range.

Our measurements are made on seven diodes with breakdown voltages between 9·5 and 46 V and with E_m between $6{\cdot}5\times10^5$ and $3{\cdot}5\times10^5$ V/cm. If (37) were not valid over the considered field range, a spread in the values of $\alpha_{n\infty}$ and b_n should be found, which is not the case.

If (37) is a bad approximation, calculated and measured reduced multiplication factors cannot be fitted for all measurements within experimental error, which is not the case (see Section 2).

Using (37), (35) becomes:

$$\Phi_n(V_k) = \Big\{1+\int_{z_{ik}}^{z_{pk}}\gamma(E_k)\alpha_{n\infty}\exp(-b_n/|E_k|)\,\mathrm{d}z\Big\} \times\Big\{\int_{z_{nk}}^{z_{ik}}\alpha_{n\infty}\exp\Big[-b_n/|E_k|-\lambda\int_{z}^{z_{ik}}\alpha_{n\infty} \times[1-\gamma(E_k)]\exp(-b_n/|E_k|)\,\mathrm{d}z'\Big]\,\mathrm{d}z\Big\} = I_k(\alpha_{n\infty},b_n), \tag{38}$$

with $k = 1, 2 \ldots m$.

As suggested by $I_k(\alpha_{n\infty}, b_n)$, the right term of (38) is only a function of $\alpha_{n\infty}$ and b_n. For a measured set of $\Phi_n(v_k)$ values, $\alpha_{n\infty}$ and b_n are determined by making a least square fit of $I_k(\alpha_{n\infty},$

b_n) to $\Phi_n(v_k)$. Therefore the function:

$$\Delta(\alpha_{n\infty}, b_n) = \frac{1}{m}\sum_{k=1}^{m} \left[\frac{\Phi_n(v_k) - I_k(\alpha_{n\infty}, b_n)}{\Phi_n(v_k)}\right]^2, \quad (39)$$

is programmed on a computer and checked for an absolute minimum with respect to $\alpha_{n\infty}$ and b_n. This method was checked by using different numerical integration methods and by varying the range of measurements and the number of measurements in the range. The function (39) was checked also for several minima. It is found that there exists only one absolute minimum for one pair of $(\alpha_{n\infty}, b)$ values.

$\alpha_n(E)$ is then given by (37) and $\alpha_p(E)$ by $\alpha_p(E) = \gamma(E)\alpha_n(E)$. Using this procedure, $\alpha_n(E)$ and $\alpha_p(E)$ are determined, using seven diodes with overlapping electric field ranges.

2. DISCUSSION OF THE IONIZATION RATES

A summary of the experimental results is given in Table 3 and in Fig. 11. The calculated values of $\alpha_n(E)$ are shown by the points around the average curve 11′ in Fig. 11. Each symbol corresponds with a particular diode as explained in Table 3. This table gives, besides the symbol used in Fig. 11, also the measured breakdown voltage of the first microplasma V_{Bm}, the breakdown voltage V_{Be} obtained by extrapolating $\Phi_n(V_a)$ to

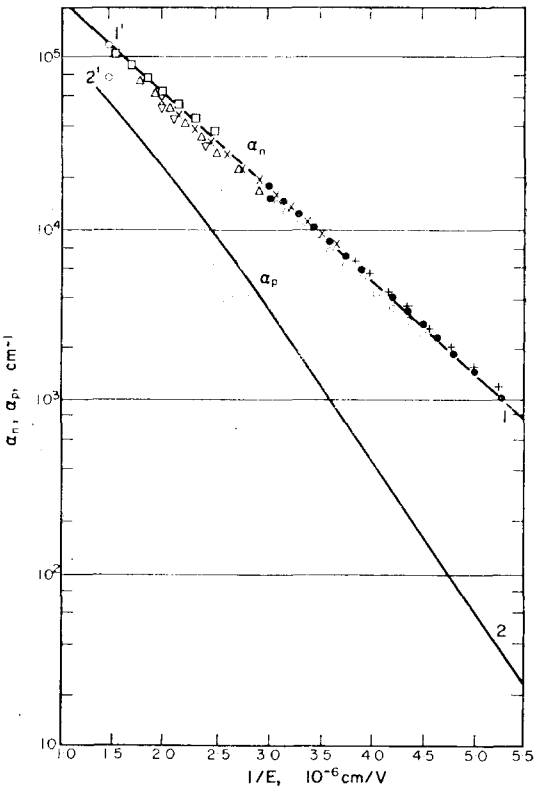

FIG. 11. The new results for the ionization rates α_n and α_p in function of the reciprocal of the electric field.
11′ : new electron data (α_n)
22′ : new hole data (α_p)
The different points around curve 11′ are discussed in Table 3.

Table 3. Results of the different measurements and calculations for the diodes used to determine $\alpha_n(E)$.

Diode no.		D 92	D IV 1	D IV 2	D III 1	D II 1	D I	D I 1
Symbol		□	△	▽	×	+	●	⊙
V_{Bm}	(V)	9·20	11·96	11·96	20·50	41·5	41·6	42·1
V_{Be}	(V)	9·50	12·40	12·40	21·40	45·2	45·3	46·0
λ	(cm)	$1{\cdot}065\times10^{-5}$	$2{\cdot}806\times10^{-5}$	$2{\cdot}806\times10^{-5}$	$1{\cdot}429\times10^{-5}$	$1{\cdot}372\times10^{-5}$	$1{\cdot}326\times10^{-5}$	$1{\cdot}317\times10^{-5}$
N_s	(cm^{-3})	$8{\cdot}187\times10^{17}$	$9{\cdot}94\times10^{17}$	$9{\cdot}94\times10^{17}$	$9{\cdot}994\times10^{16}$	$1{\cdot}853\times10^{16}$	$1{\cdot}799\times10^{16}$	$1{\cdot}825\times10^{16}$
N_{sr}	(cm^{-3})	—	$9{\cdot}50\times10^{17}$	$9{\cdot}50\times10^{17}$	$1{\cdot}10\times10^{17}$	$1{\cdot}80\times10^{16}$	$1{\cdot}80\times10^{16}$	$1{\cdot}9\times10^{16}$
a	(cm^{-4})	$7{\cdot}691\times10^{22}$	$3{\cdot}544\times10^{22}$	$3{\cdot}544\times10^{22}$	$6{\cdot}993\times10^{21}$	$1{\cdot}351\times10^{21}$	$1{\cdot}356\times10^{21}$	$1{\cdot}388\times10^{21}$
E_1	(V cm^{-1})	$4{\cdot}171\times10^{5}$	$3{\cdot}437\times10^{5}$	$3{\cdot}880\times10^{5}$	$2{\cdot}757\times10^{5}$	$1{\cdot}906\times10^{5}$	$1{\cdot}897\times10^{5}$	$2{\cdot}141\times10^{5}$
E_m	(V cm^{-1})	$6{\cdot}494\times10^{5}$	$6{\cdot}185\times10^{5}$	$5{\cdot}767\times10^{5}$	$4{\cdot}830\times10^{5}$	$3{\cdot}372\times10^{5}$	$3{\cdot}347\times10^{5}$	$3{\cdot}490\times10^{5}$
ϵ_m	(%)	0·91	0·86	0·33	1·35	2·55	2·55	0·92
$\alpha_{n\infty}$	(cm^{-1})	$6{\cdot}60\times10^{5}$	$7{\cdot}10\times10^{5}$	$6{\cdot}75\times10^{5}$	$5{\cdot}20\times10^{5}$	$6{\cdot}10\times10^{5}$	$6{\cdot}20\times10^{5}$	$5{\cdot}60\times10^{5}$
b_n	(V cm^{-1})	$1{\cdot}161\times10^{6}$	$1{\cdot}282\times10^{6}$	$1{\cdot}260\times10^{6}$	$1{\cdot}130\times10^{6}$	$1{\cdot}189\times10^{6}$	$1{\cdot}186\times10^{6}$	$1{\cdot}200\times10^{6}$

$\Phi_n = 1$, the profile parameters λ and N_s determined from capacitance measurements, N_{sr} determined by resistivity measurements and the impurity gradient a determined from capacitance measurements, for the different diodes. The fields E_1 and E_m are the maximum electric fields, respectively for the lowest voltage V_1 and the highest voltage V_m. They give approximately the range of validity of the measurements. The minimal mean error $\epsilon_m = [\Delta(\alpha_{n\infty}, b_n)]^{1/2}$ on the fitting with the $\Phi_n(V_a)$ curve and the values of $\alpha_{n\infty}$ and b_n corresponding to this minimal error are also listed in Table 3.

Figure 11 also shows $\alpha_p(E)$ by curve 22', obtained from $\alpha_p(E) = \gamma(E).\alpha_n(E)$.

The discrepancy between the measured breakdown voltage V_{Bm} and the extrapolated breakdown voltage V_{Be} is due to the influence of microplasmas. In appendix C experimental evidence is given that microplasmas have a completely negligible effect on the measured multiplication factors as long as V_a is smaller than V_{Bm}. This means that ionization rates measured on diodes with some microplasmas must be the same as those measured on microplasma free diodes as already mentioned in Ref. 1. The breakdown voltage V_{Be}

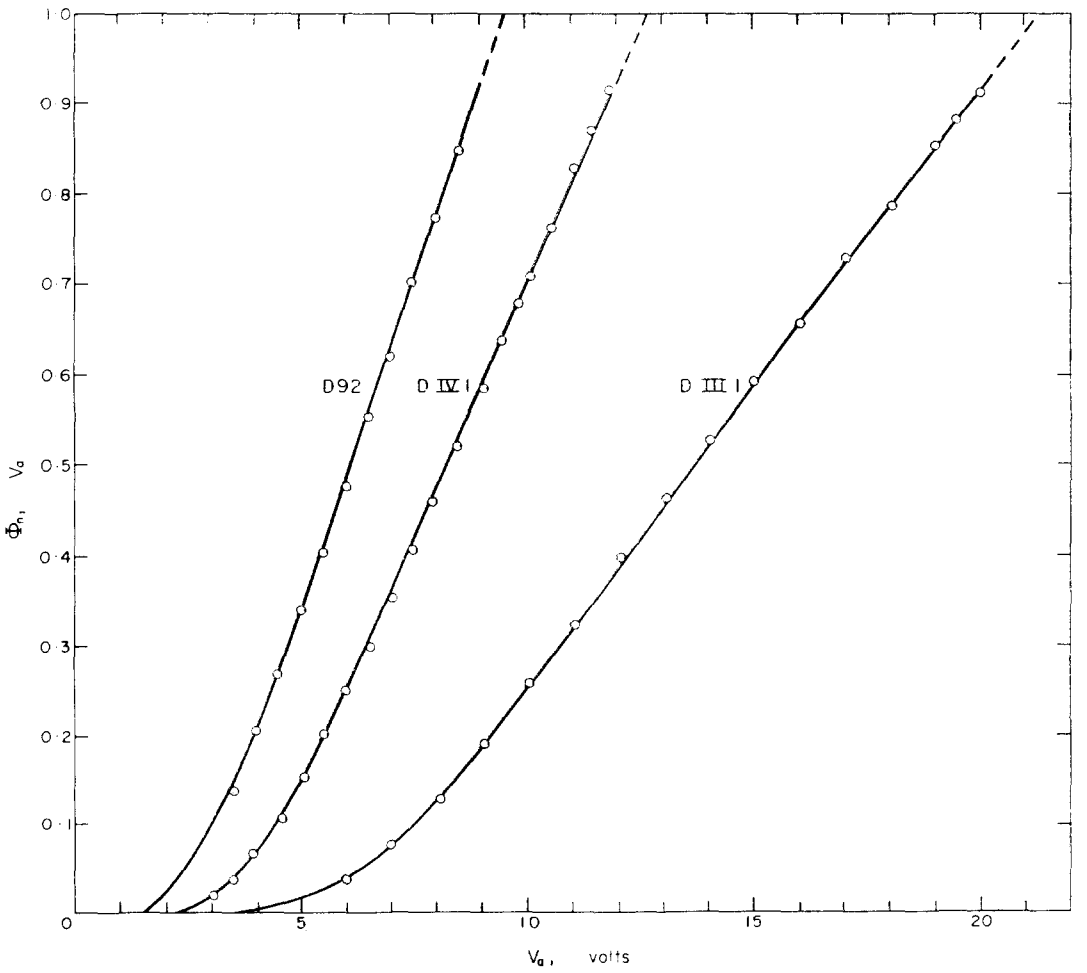

FIG. 12. Comparison of the measured reduced multiplication factor $\Phi_n(V_a)$ (points ⊙) with the computed ionization integral for diodes D 92, D IV 1 and D III 1.

obtained by extrapolating the $\Phi_n(V_a)$ curve to $\Phi_n(V_{Be}) = 1$ is the one that must be compared with the breakdown voltage computed from the measured $\alpha_p(E)$ and $\alpha_n(E)$ values (see Section 3).

The agreement between the value N_s of substrate concentration obtained from capacitance measurements and the value N_{sr} obtained from a resistivity measurement is very good.

The mean error ϵ_m between the measured $\Phi_n(V_a)$ and the one calculated from $\alpha_{n\infty}$ and b_n is always less than 2·6 per cent for all diodes. Figure 12 shows an example of this fitting for three diodes (D 92, D IV 1 and D III 1). The curves are calculated with an IBM 360 from $\alpha_{n\infty}$ and b_n listed in Table 3; the points are the experimental values. The good agreement between the measurements and the calculations proves the validity of Chynoweth's law in the restricted field range of each diode. From Table 3 we also remark that the values $\alpha_{n\infty}$ and b_n for all diodes are nearly the same and we conclude that Chynoweth's law is a good approximation in the whole field range covered by the set of measured diodes.

The results of Fig. 11 are different from those of Refs. 1 and 2 essentially by the slope (compare with Fig. 1). Indeed, the equation of the average curve (1) for $\alpha_n(E)$ is

$$\alpha_n = \alpha_{n\infty} \exp(-b_n/|E|)$$

where $\alpha_{n\infty} = 7{\cdot}03 \times 10^5$ cm^{-1} and $b_n = 1{\cdot}231 \times 10^6$ V cm^{-1} while in Ref. 1, one finds

$\alpha_{n\infty} = 1{\cdot}6 \times 10^6$ cm^{-1} and $b_n = 1{\cdot}65 \times 10^6$ Vcm^{-1}

and in Ref. 2

$\alpha_{n\infty} = 3{\cdot}36 \times 10^6$ cm^{-1} and $b_n = 1{\cdot}75 \times 10^6$ Vcm^{-1}.

The difference in $\alpha_{n\infty}$ is of secondary importance, since this results from the difference in b_n to give about the same value of α_n in the given field range. The discrepancy of the slope in Ref. 1 is caused by not taking into account the influence of the threshold energy ϵ_i for electrons, which is necessary

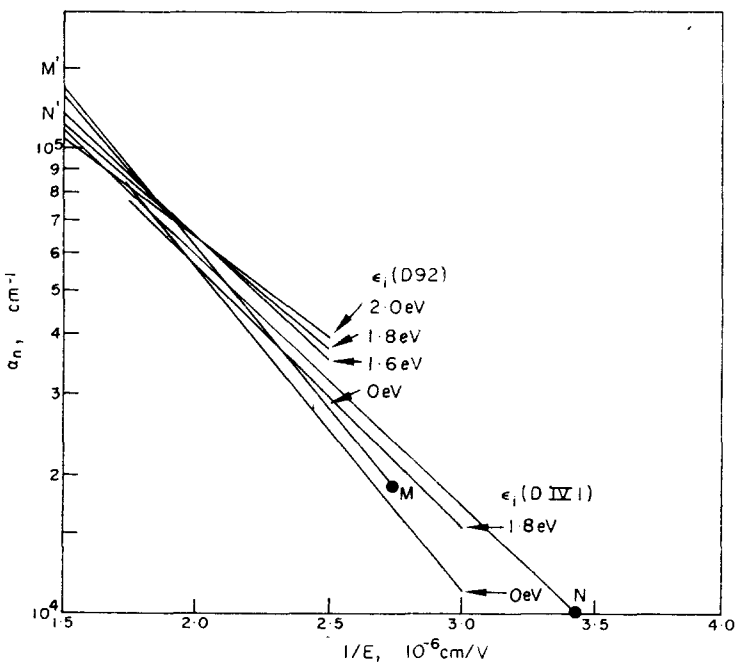

FIG. 13. The influence of the correction for the threshold energy ϵ_i on the slope of log α_n $(1/E)$.

NN′ : our average data for low fields
MM′ : data of MOLL and VAN OVERSTRAETEN[1].

since narrow junctions are used. This is illustrated by Fig. 13. With the data of D 92, used in Ref. 1, α_n is calculated for $\epsilon_i = 0$; 1·6; 1·8 and 2 eV as explained in Section 1.4.c, and is shown in Fig. 13. The slope of α_n decreases with increasing ϵ_i. The slope nearly coincides with our average data NN′ for low fields, for $\epsilon_i = 1{\cdot}8$ eV. This may be a confirmation for the value $\epsilon_i = 1{\cdot}8$ eV given in Ref. 1. For $\epsilon_i = 0$ eV the curve nearly coincides with the data of Moll and Van Overstraeten represented in Fig. 13 by MM′, indicating that their assumption of a constant γ value has not strongly affected their high field values for $\alpha_n(E)$.

The same procedure is used for diode D IV 1 ($V_{Be} = 12{\cdot}4$ V) for $\epsilon_i = 0$ and $\epsilon_i = 1{\cdot}8$ eV. This gives the same result. No correction for the threshold energy is needed for diodes with a breakdown voltage higher than 20 V. This is illustrated clearly by Figs. 14 and 15. Figure 14 gives the field distribution in D 92 ($V_B = 9{\cdot}2$ V) for $V_a = 8{\cdot}5$ V, and the calculated $\alpha_n(E)$ and $\alpha_p(E)$ curves. The distance x_p–x_i, for an electron to get the energy ϵ_i is an important part of the total junction width $w = x_p$–x_n, and the shaded area ($x_i A x_p$), being approximately the part of the ionization integral ineffective for ionization, is important. This requires a larger ionization coefficient $\alpha_n(E)$ in the remaining part of the junction in order to obtain the same integral. The correction increases with decreasing bias, since $(x_i - x_p)/(x_p - x_n)$ increases with decreasing voltages.

Figure 15 is analoguous to Fig. 14, but for the diode D I 1 (with $V_{Bm} = 42{\cdot}1$ V) and for $V_a = 32{\cdot}2$ V. It should be remarked, that the field distribution is almost abrupt and that in the non-effective part $x_i A x_p$, the values of $\alpha_n(E)$ are more than an order of magnitude smaller than in the rest of the depletion region and the ineffective part of the ionization integral is completely negligible. The computation with and without the correction for threshold gives the same result.

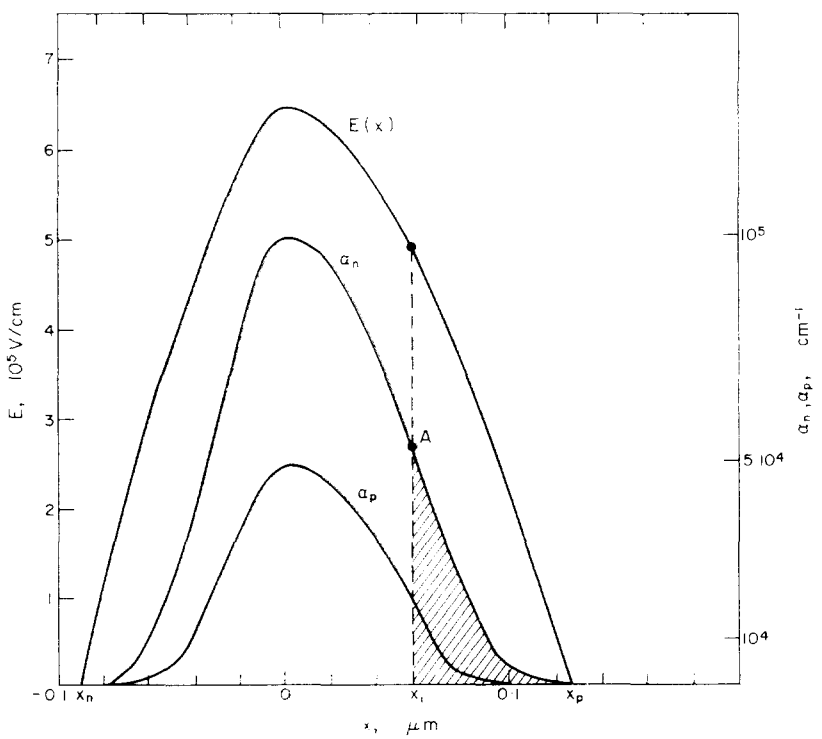

FIG. 14. Ionization rates α_n and α_p and electric field $E(x)$ in the depletion region of diode D 92 at $V_a = 8{\cdot}5$ V.

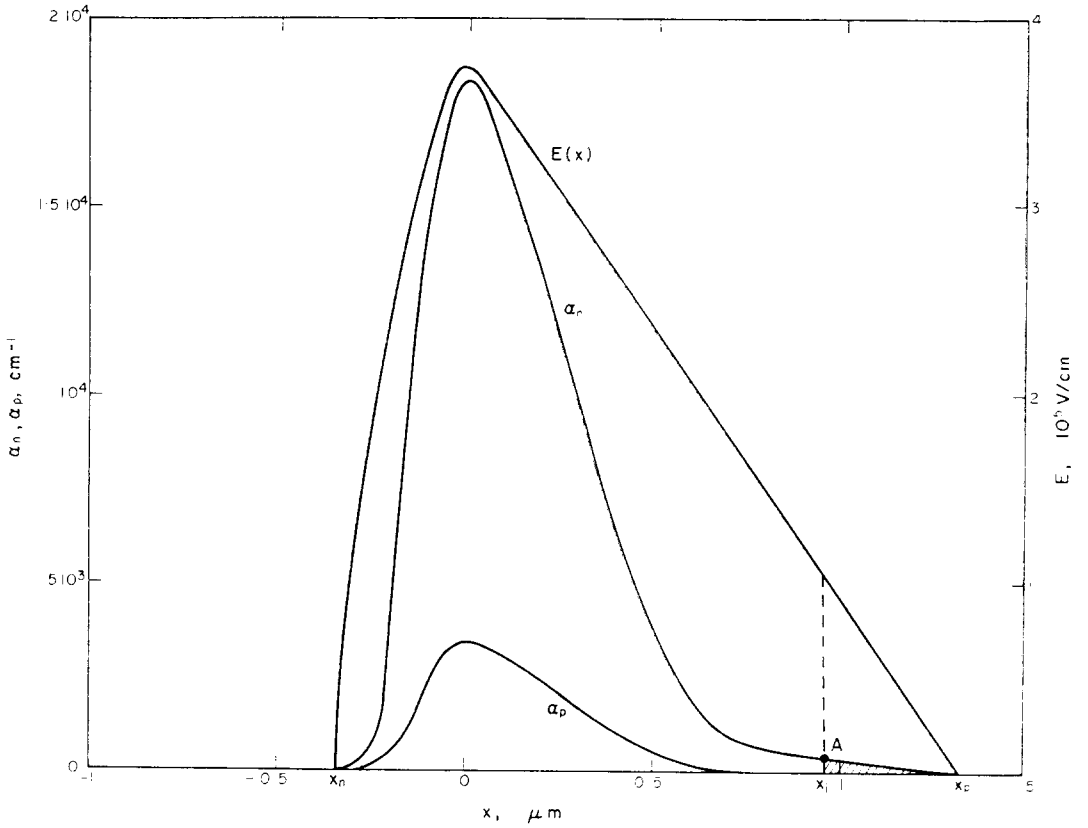

FIG. 15. Ionization rates α_n and α_p and electric field $E(x)$ in the depletion region of diode D I 1 at $V_a = 32{\cdot}2$ V.

Concerning the difference between our results for α_n and α_p with those of LEE, LOGAN *et al.*,[2] we can make the following remarks:

For their diode 6 AG 35 with a breakdown voltage of 6 V the authors make no correction for the threshold energy. As already shown, such corrections are necessary for diodes with breakdown voltages lower than 20 V.*

From their depletion layer width as a function of the voltage and the value $\lambda \approx 7 \times 10^{-5}$ cm for diode 29–9, it is possible to calculate the gradient ($a = 1{\cdot}37 \times 10^{21}$ cm^{-4}) and the electric field distribution for this diode. Starting from their multiplication data we also computed $\alpha_{n\infty}$ and b_n using our method. This yields:

$$\alpha_{n\infty} = 9{\cdot}4 \quad \times 10^5 \text{ cm}^{-1}$$

$$b_n = 1{\cdot}295 \times 10^6 \text{ V cm}^{-1}$$

in good agreement with our results.

The electron multiplication factors, computed from LEE, LOGAN *et al.*'s data and from our data are represented respectively by curve 2 and the points around the measured curve 1 in Fig. 16. The discrepancy between curve 2 and curve 1 is clearly due to a too steep slope of the ionization rates. We believe this to be due to inaccuracies in numerically solving Abel's integral equation in which it is necessary to differentiate measured

* For a diode with $V_B = 6$ v, the gradient a is of the order of 10^{24} cm^{-4} (Section 3). For the minimum junction voltage of $V = \epsilon_i/q = 1{\cdot}8$ V; the electric field equals approximately $E_m = (9\,qa/32\,\epsilon)^{1/3}\,V^{2/3} = 5{\cdot}2 \times 10^5$ V cm^{-1}, which is already higher than the maximum electric field ($4{\cdot}08 \times 10^5$ V cm^{-1}) for which an electron ionization rate is given by the authors. This can be due to an error in the calculation of the maximum electric field.

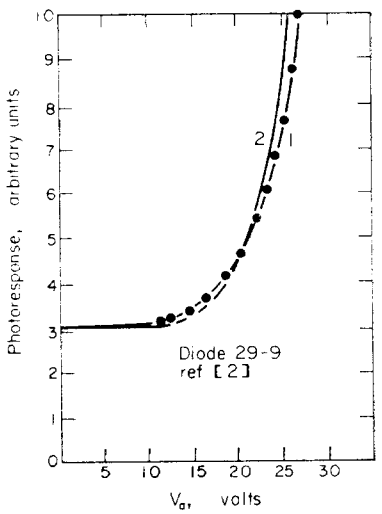

FIG. 16. Measured and computed photo response for diode unit 29-9.

Curve 1: electron initiated photo current as measured in ref. 2 on the diode 29-9. The points are computed with (4) and our ionzation data.

Curve 2: is computed with the data of LEE, *et al.*[2]

functions. This difficulty is avoided in a least square method.

3. CALCULATION OF BREAKDOWN VOLTAGES

3.1. *Breakdown voltage of diffused p–n and p–i–n. junctions*

In this section the breakdown voltages of diffused mesa *p–n* junctions will be calculated, using our $\alpha_n(E)$ and $\gamma(E)$ data discussed in the preceding section. The diffusion profile again is approximated by the exponential profile given by (5). The breakdown voltage V_B can be derived from the condition:

$$\Phi_n(V_B)-1=0. \tag{40}$$

Using (4) and the notations and values discussed in Section I.2.b, (40) becomes:

$$\lambda\alpha_{n\infty}\int_{z_n(v)}^{z_p(v)}\exp\Big\{-b_n/|E(z)|-\lambda\alpha_{n\infty}\int_{z}^{z_p(v)}[1-\gamma(E(z'))]\times\exp(-b_n/|E(z')|\,dz'\Big\}\,dz-1=0. \tag{41}$$

It is convenient to calculate V_B as a function of the substrate concentration N_s and of the impurity gradient a at the metallurgical junction. A set of values v_k for the reduced voltage v is chosen. For each v_k we calculate the boundaries z_{pk} and z_{nk} (equation (7) and (8)) and we chose a set of values E_{mj} for the maximum electric field in the junction. With each E_{mj} and with a certain value of v_k corresponds a value E_{0jk} for E_0 given by equation (13). With these values of z_{nk}, z_{pk} and E_{0jk} (41) is only an equation in λ, which can be solved using the Müllers—S—iteration method and a special form of Gauss quadrature for computing the integrals. Let λ_{jk} be the solution of (41). The breakdown voltage V_{Bjk} is then given by (10), or

$$V_{Bjk}=\lambda_{jk}E_{0jk}v_k-V_d.$$

The substrate concentration N_{sjk} and the gradient a_{jk} corresponding to the given values E_{0jk} and v_k are given by (11) and (5a), or

$$N_{sjk}=\epsilon E_{0jk}/q\lambda_{jk}.$$

$$a_{jk}=N_{sjk}/\lambda_{jk}.$$

The width of the junction at breakdown is given by:

$$w_{jk}=\lambda_{jk}(z_{pk}-z_{nk}).$$

Using this method, breakdown voltages are computed for

$$1{\cdot}6\times10^5\leqslant E_{mj}\leqslant 10^6\ \mathrm{V\ cm^{-1}}.$$

Figure 17 shows the computed breakdown voltages V_B* below 160 V as a function of the substrate concentration and with the gradient a as a parameter. Also curves with constant junction width w_B at breakdown are given. These may be important for calculations of the capacitance

$$C=\epsilon A/w_B$$

at the breakdown voltage of microwave avalanche diodes. The breakdown voltages are in good agreement with earlier calculations of SZE and GIBBONS[13] calculated with the data of LEE, LOGAN *et al.* probably because the absolute values of the new data at the high electric field range do not differ strongly from the data of LEE, LOGAN *et al.*

The breakdown voltages, V_B, increased by the built in voltage V_d, of some low voltage phosphorus

* From these curves the built in voltage V_d must be substracted to find the measured breakdown voltage.

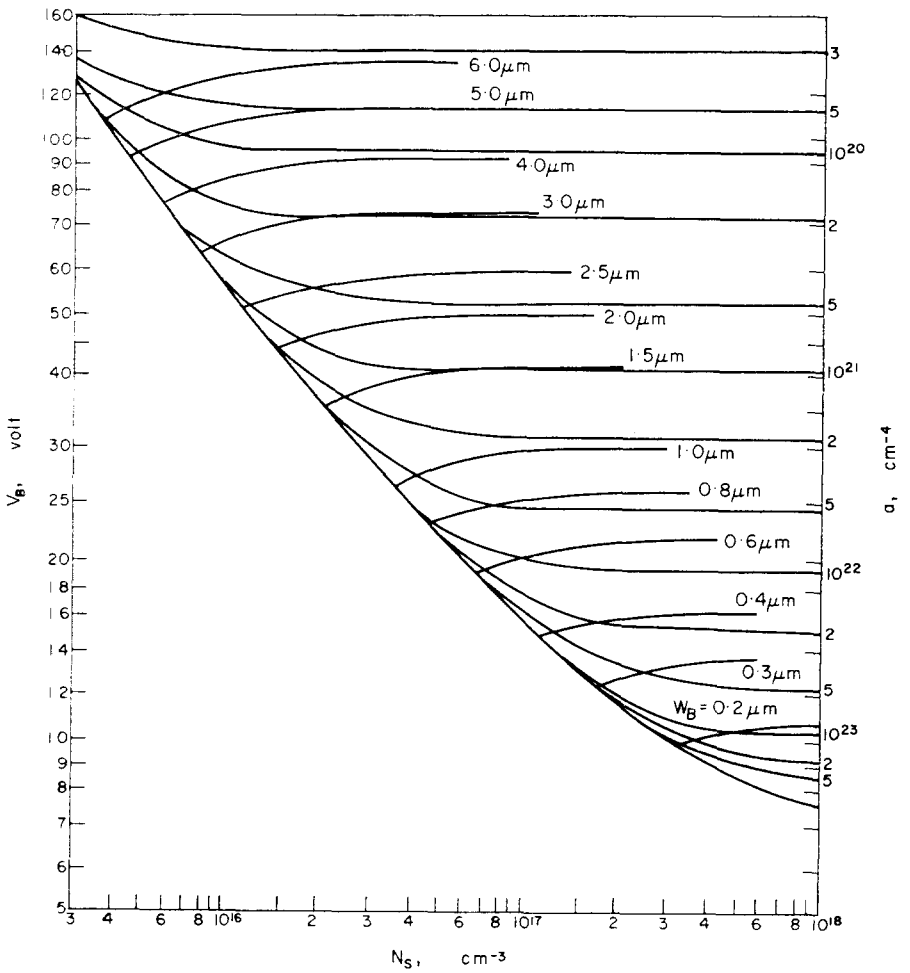

FIG. 17. The breakdown voltage V_B of diffused mesa diodes versus the substrate concentration N_s, within the range $3\times10^{15} \leqslant N_s \leqslant 10^{18}$ cm^{-3} and with the gradient a as parameter. Also curves of constant junction width w_B at breakdown are shown.

diffused mesa junctions are measured by extrapolating the reduced multiplication curve to $\Phi_n(V_B) = 1$ in order to eliminate microplasma effects. They are listed in Table 4 together with the parameters N_s and a (from capacitance measurements) and the breakdown voltage V_{Bc} found from Fig. 17. The agreement between the measured and the calculated values seems to be very good. Of more interest are the calculations for high voltage devices shown in Fig. 18. The upper right side of this figure is valid for mesa diffused p–n diodes and gives the breakdown voltage up to $1{\cdot}6\times10^4$ V as a

Table 4. Comparison between the measured breakdown voltage V_B and the computed one, V_{Bc}.

Diode	a cm^{-4}	N_s cm^{-3}	V_B V	V_{Bn} V
D 92	$7{\cdot}69\times10^{22}$	$8{\cdot}19\times10^{17}$	10·22	11·0
D IV 1	$3{\cdot}54\times10^{22}$	$9{\cdot}94\times10^{17}$	13·07	13·3
γ_{00}	$1{\cdot}70\times10^{22}$	8×10^{17}	16·53	16·2
D III 1	$6{\cdot}99\times10^{21}$	$9{\cdot}99\times10^{16}$	22·05	22·5
γ_{02}	$2{\cdot}25\times10^{21}$	$5{\cdot}00\times10^{16}$	31·94	32·0
D II 1	$1{\cdot}35\times10^{21}$	$1{\cdot}85\times10^{16}$	45·80	44·0
γ_{00}	$1{\cdot}60\times10^{20}$	$3{\cdot}25\times10^{15}$	119·5	122·0

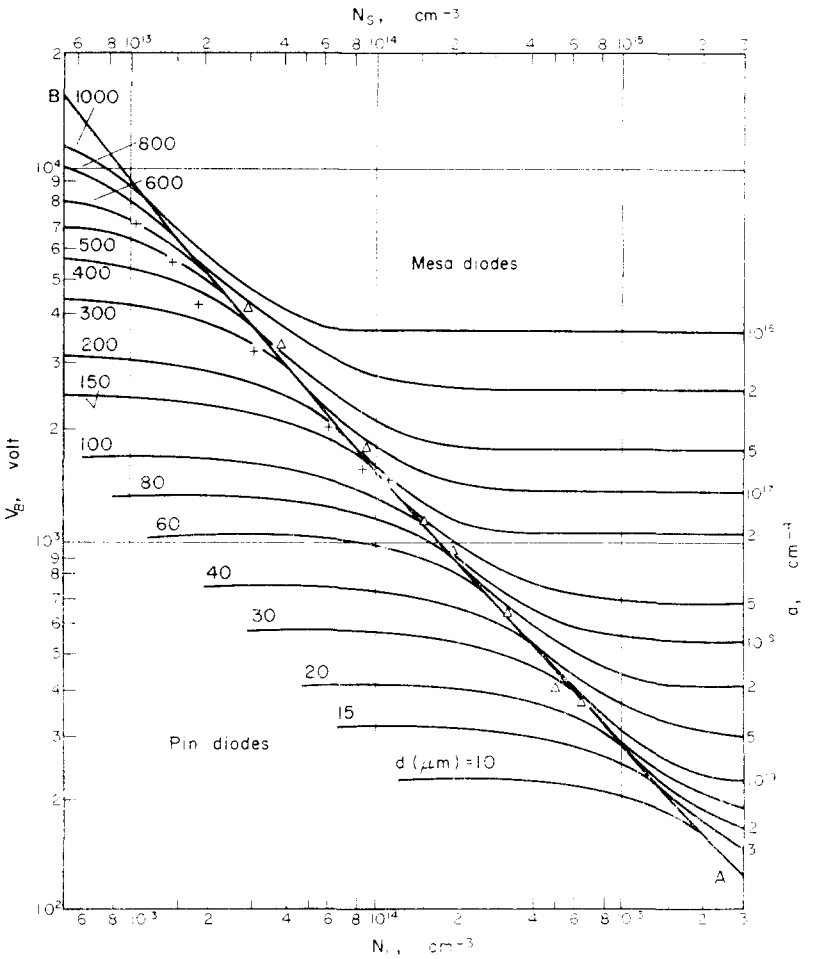

FIG. 18. The breakdown voltage V_B of diffused mesa diodes (upper right) vs. the substrate concentration N_s, within the range $3\times10^{12} \leqslant N_s \leqslant 3\times10^{15}\,\mathrm{cm}^{-3}$, and with the gradient a as parameter. The left curves show the breakdown voltage of $p^+\,i\,n^+$ diodes vs. the concentration of the i—zone N_i and with the width of the i—region as parameter.

function of the substrate concentration N_s with the gradient a as parameter. The curve AB is valid for quasi-abrupt junctions. This curve has to be compared with the measurements of KOKOSA and DAVIES[3] on diffused p^+n junctions (indicated by small triangles) and of MONCH[14] on diffused n^+p junctions (indicated by + signs). The agreement with the data of Kokasa and Davies is very good. For low substrate concentrations the measurements of Monch are lower than the calculated values but the author is in doubt about the correct values of his substrate concentrations. This comparison is interesting because Kokosa and Davies remark that the existing ionization rates do not fit their experimental values. The agreement of the new ionization data with these measurements is an indication for their reliability.

Because most high-voltage power diodes are of the $p^+i\,n^+$ type we also computed breakdown voltages of such diodes assuming the p^+i and $i\,n^+$

junctions of the abrupt type. Therefore we take the thickness d and the concentration N_i of the low doped middle zone as parameters. The computed breakdown voltages V_B are represented in Fig. 18 as a function of N_i with the thickness d as parameter (curves at the lower left part of the curve AB). These curves indicate that, for a given d, a lowering of the concentration N_i does not change the breakdown voltage appreciably, which can be of interest for the choice of the starting material for making such devices.

3.2. *Introduction of an effective ionization rate* $\alpha_{eff}(E)$

Many authors[3,16] introduce an effective ionization rate $\alpha_{eff}(E)$, equal for electrons and holes and use it for breakdown calculations. As already mentioned by KOKOSA and DAVIES[3] this is indeed possible if the ratio $\gamma = \alpha_p/\alpha_n$ is a constant. In this case, they prove that breakdown occurs if:

$$1 - \int_{x_n}^{x_p} \frac{\gamma - 1}{\ln\gamma} \alpha_n(E)\, dx = 0, \qquad (42)$$

or if one puts:

$$\alpha_{eff} = \frac{\gamma - 1}{\ln\gamma} \alpha_n(E), \qquad (43)$$

(42) becomes:

$$1 - \int_{x_n}^{x_p} \alpha_{eff}(E)\, dx = 0. \qquad (44)$$

We have seen in Section 1.4.b that γ is a function of the electric field, as described by (34). We now make the hypothesis that (43) should also be valid if γ is a function of E and we calculate $\alpha_{eff}(E)$ from the measured $\gamma(E)$ and $\alpha_n(E)$ values. Plotting log α_{eff} vs. $1/E$ results in practically a straight line, which may be represented by:

$$\alpha_{eff}(E) = 7.03 \times 10^5 \exp(-1.468 \times 10^6/|E|) \qquad (45)$$

The breakdown voltages calculated using (45) in (44) are somewhat lower than the exact values calculated in the preceding section. The maximum deviation however is smaller than 3 per cent and if this tolerance is permitted the calculation of breakdown voltages can be greatly simplified using the breakdown condition (44) and the expression (45) for $\alpha_{eff}(E)$. It is worth noticing that the effective ionization coefficient α_{eff} may be used for breakdown voltage calculations but not for multiplication calculations since herewith the injection ratio k and the ratio $\gamma = \alpha_p/\alpha_n$ play an important role.

CONCLUSIONS

The field dependence of the ionization rates for electrons and holes is computed from the measurement of charge multiplication in silicon p–n junctions.

The ionization rates satisfy Chynoweth's law and can be approximated by:

(1) electrons:

$$\alpha_n(E) = 7{\cdot}03 \times 10^5 \exp(-1{\cdot}231 \times 10^6/|E|)\ \text{cm}^{-1}$$
$$\text{for } 1{\cdot}75 \times 10^5 \leqslant E \leqslant 6{\cdot}40 \times 10^5\ \text{V cm}^{-1}$$

(2) holes:

$$\alpha_p(E) = 1{\cdot}582 \times 10^6 \exp(-2{\cdot}036 \times 10^6/|E|)\ \text{cm}^{-1}$$
$$\text{for } 1{\cdot}75 \times 10^5 \leqslant E \leqslant 4 \times 10^5\ \text{V cm}^{-1}$$

and

$$\alpha_p(E) = 6{\cdot}71 \times 10^5 \exp(-1{\cdot}693 \times 10^6/|E|)\ \text{cm}^{-1}$$
$$\text{for } 4 \times 10^5 \leqslant E \leqslant 6{\cdot}40 \times 10^5\ \text{V cm}^{-1}$$

These ionization rates differ from the data of MOLL and VAN OVERSTRAETEN[1] because they neglect the influence of the threshold energy ϵ_i for electrons. The data of LEE, *et al.*[2] are different for the same reason, and it is also proved that their ionization rates are not compatible with their measured multiplication factors due to a too steep slope of their data, possibly caused by numerical inaccuracies.

For practical purposes breakdown voltages of p–n and p–i–n diodes are calculated. The breakdown voltages computed from the new ionization rates are in agreement with experiments. As shown by Kokosa and Davies this agreement, especially for high voltage devices, did not exist with the previous ionization data.

An effective ionization rate $\alpha_{eff}(E)$, suitable for the calculation of breakdown voltages and obeying Chynoweth's law is introduced and given by:

$$\alpha_{eff}(E) = 7{\cdot}03 \times 10^5 \exp(-1{\cdot}468\ 10^6/|E|)\ \text{cm}^{-1}$$
$$\text{for } 1{\cdot}75 \times 10^5 \leqslant E \leqslant 6{\cdot}40 \times 10^5\ \text{V cm}^{-1}.$$

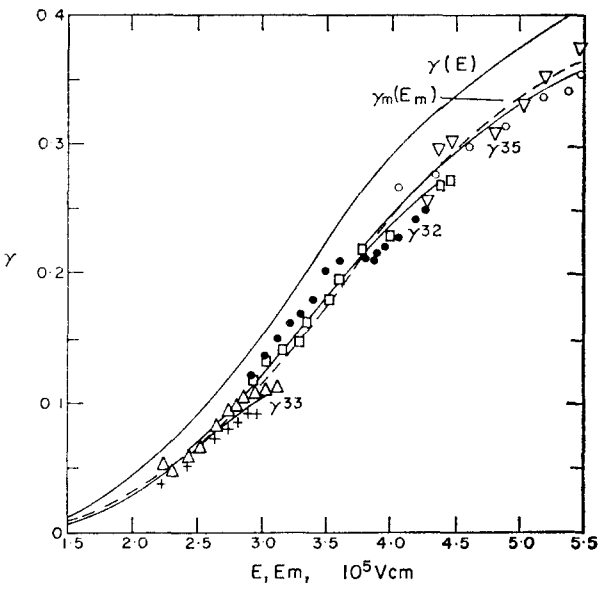

FIG. 19. Verification of the constant $c = 0{\cdot}9$ for the determination of $\gamma(E)$.

$\Delta, +, \bullet, \square, \circ, \nabla$: γ values in function of $E_m(V)$, calculated from measured $M_n(V)$ and $M_p(V)$.

$\gamma_m(E_m)$: mean curve through the measured values.

$\gamma(E)$: curve computed from the measured $\gamma_m(E_m)$ curve by replacing E_m by $E = 0{\cdot}9\,E_m$.

$\gamma_{32}, \gamma_{33}, \gamma_{35}$: $\gamma(E_m)$ curves computed from the $\gamma(E)$ curve and the measured $\alpha_n(E)$ function.

Acknowledgements—The authors wish to express their gratitude to Ir. P. DETOURNEY for writing most of the computer programs and to the computer center of the Catholic University of Louvain for executing them. They also thank Ir. W. NUYTS for many helpful discussions.

REFERENCES

1. J. L. MOLL and R. VAN OVERSTRAETEN, *Solid-St. Electron.* **6,** 147 (1963).
2. C. A. LEE, R. A. LOGAN, R. L. LATDORF, J. J. KLEIMACK and W. W. WIEGMANN, *Phys. Rev.* **134,** A 761 (1964).
3. R. A. KOKOSA and R. L. DAVIES, *IEEE Trans. Electron. Devices* **ED-13,** 874, (1966).
4. F. VAN DE WIELE, R. VAN OVERSTRAETEN and H. DE MAN, *Solid-St. Electron.* **13,** 25 (1970).
5. R. M. BURGER and R. P. DONOVAN, *Fundamentals of Silicon integrated device technology*, Vol. I, pp. 236–253. Prentice Hall, New Jersey, (1967).
6. W. C. DUNLAPP and R. L. WATTERS, *Phys. Rev.* **92,** 1396 (1953).
7. W. C. DASH and R. NEWMAN, *Phys. Rev.* **99,** 1151 (1955).
8. A. BILLOTTI, *Solid-St. Electron.* **10,** 445 (1967).
9. J. L. MOLL, *Physics of Semiconductors*, p. 192. Mc-Graw Hill, New York (1964).
10. J. R. HAYNES and W. C. WESTPHAL, *Progress in Semiconductors*, Vol. I, p. 24. Haywood, London, (1956).
11. I.B.M. Subroutines QG 10 and R.T.M.I.
12. S. L. MILLER, *Phys. Rev.* **99,** 1234 (1955).
13. S. M. SZE and G. GIBBONS, *Appl. Phys. Lett.* **8,** 111 (1966).
14. W. MONCH, *Solid-St. Electron.* **10,** 1085 (1967).
15. R. H. HAITZ, A. GOETZBERGER, R. M. SCARLETT and W. SCHOCKLEY, *J. appl. Phys.* **34,** 1581, (1963).
16. T. OGAWA, *J. appl. Phys.*, Japan, **4,** 473, (1965).

APPENDIX A

In Section 1.4.b, it is mentioned that the γ value computed from (31) at a given voltage V has to be associated to an electric field $E = cE_m$ with c close to unity. The dotted curve $\gamma_m(E_m)$ in Fig. 19 is the mean curve through the values computed from the measured $M_p(V)$ and $M_n(V)$. The field dependence of γ is computed from the measured $\gamma_m(E_m)$ curve, simply by replacing E_m by $E = (c = 0{\cdot}9)xE_m$, and is shown in Fig. 19 by the γ (E) curve.

The curves γ_{33}, γ_{32} and γ_{35} are computed from $\gamma(E)$ and the measured $\alpha_n(E)$ function for three diodes. These curves are in good agreement with the mean curve $\gamma_m(E_m)$ indicating that the value $c = 0{\cdot}9$ is the correct one. Using another c gives a parallel shift to the curves γ_{33}, γ_{32} and γ_{35} making the fitting between theory and experiment impossible.

APPENDIX B

In Ref. 2 it is proved that:

$$\exp\left[-\int_{x_n}^{x_p}(\alpha_n-\alpha_p)\,dx\right] = M_p/M_n. \qquad (B.1)$$

Introducing (B.1) and (4) into (1a) one finds for nearly pure electron injection with an injection ratio $k = J_{np}/J_{pn}$:

$$M_e = \frac{M_p/M_n+k}{1+k}M_n, \qquad (B.2)$$

or:

$$M_p+kM_n = (1+k)M_e. \qquad (B.3)$$

Introducing (B.1) and (3) into (1b) one finds for nearly pure hole injection with an injection ratio $k' = J_{pn}/J_{np}$:

$$M_h = \frac{M_n/M_p+k'}{1+k'}M_p \qquad (B.4)$$

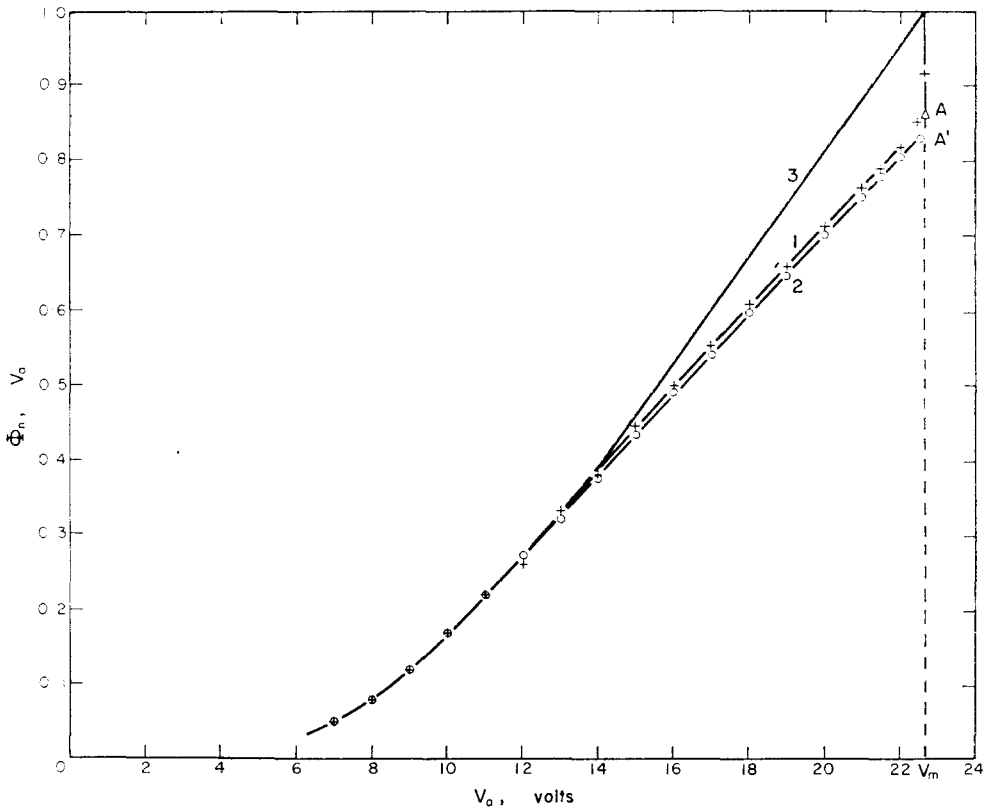

FIG. 20. The influence of a microplasma on the reduced charge multiplication $\Phi_n(V_a)$.

Curve 1	: $\Phi_n(V_a)$ with a lightspot of 20 μm on the microplasma
Curve 2 and point A	: $\Phi_n(V_a)$ with the lightspot of 20 μm outside the microplasma
Curve 2 and point A'	: $\Phi_n(V_a)$ of the completely illuminated junction
Curve 3	: probable $\Phi_n(V_a)$ for the micro-plasma alone

or:

$$k'M_p + M_n = (1+k')M_h \qquad \text{(B.5)}$$

M_n and M_p solved from (B.3) and (B.5), introduced into equation (31) yields the result

$$\gamma = \frac{k(1+k')M_h - (1+k)M_e - kk' + 1}{k'(1+k)M_e - (1+k')M_h - kk' + 1} \qquad \text{(B.6)}$$

mentioned in Section 1.4.b.

APPENDIX C

The influence of microplasmas has been disputed in the past.[2] To study this influence, multiplication measurements are made on a diode which shows very marked microplasma noise. The microplasma could be localized by illumination with a 20 μ microscope lightspot because the microplasma is turned on continuously by the injection of charge carriers, and the noise disappears. The electron multiplication factor M_n was measured under several circumstances: with a small lightspot focused on the microplasma, with a small lightspot focused outside the microplasma, with the whole diode outside the microplasma illuminated and with the whole area illuminated. The results of measurements of the reduced multiplication factor Φ_n vs. the applied voltage V_a are shown in Fig. 20. It should be remarked that:

The lack of microplasma noise by illumination of the microplasma excludes that other microplasmas are active at this voltage.

Curve 1 of Fig. 20, giving $\Phi_n(V_a)$ for the microplasma itself, is only insignificantly different from curve 2, valid for the other cases, except around V_m, the turn-on voltage of the microplasma.

Illumination with a 20 μm lightspot outside the microplasma gives a $\Phi_n(V_a)$ curve which coincides,

except for point A, with the curves corresponding to a completely illuminated junction and to a junction completely illuminated except for the microplasma. This is caused by the fact that the multiplied saturation current becomes comparable to the small multiplied photo current at point A.

Hence we may conclude that the presence of microplasmas makes the measurement of multiplication factors up to the theoretical breakdown voltage V_B impossible, but that the multiplication factor below the turn-on voltage V_m of the microplasma is not influenced by it. This conclusion can also be derived from the multiplication measurements cited in Ref. 15.

One concludes that the ionization rates derived from the measured multiplication in diodes with microplasmas must be equal to those measured on microplasma free diodes, or that calculations with such ionization rates must yield correct results for microplasma free diodes.